

Optimized chiral hamiltonians for practical use: - current status and perspectives

Andreas Ekström (Oslo University, Norway and
Chalmers University of Technology, Sweden)

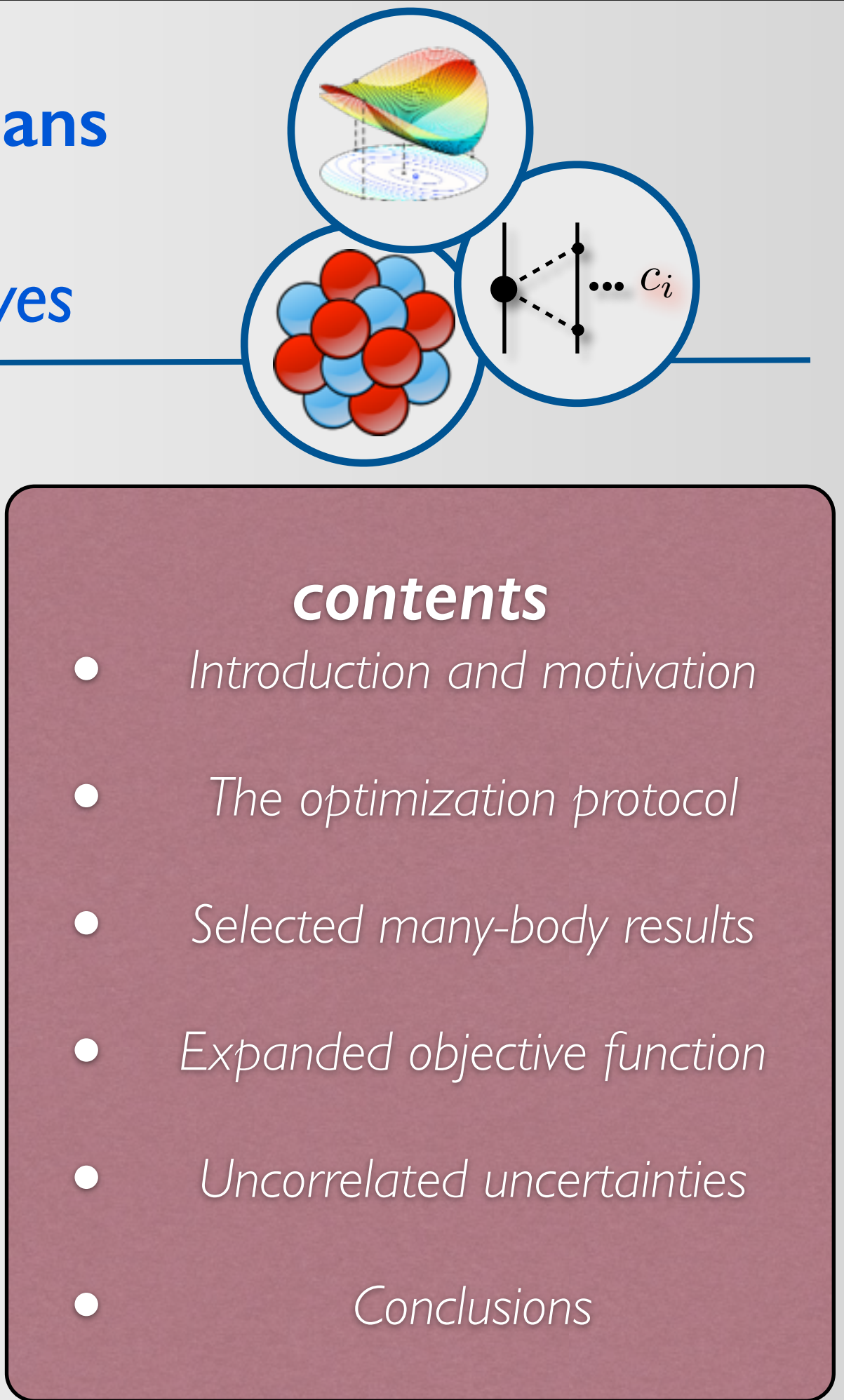
Collaborators:

Gustav Baardsen (UiO)
Boris Carlsson (UiO/Chalmers)
Christian Forssen(Chalmers)
Gaute Hagen(ORNL)
Morten Hjorth-Jensen(UiO/MSU)
Gustav Jansen(UT/ORNL)
Ruprecht Machleidt(UI)
Witold Nazarewicz(UT/ORNL)
Thomas Papenbrock(UT/ORNL)
Jason Sarich(ANL)
Kyle Wendt(UT/ORNL)
Stefan Wild(ANL)

TRIUMF Workshop

"Nuclear Structure & Reactions : Experimental and Ab Initio Theoretical Perspectives"

February 18-21, 2014, TRIUMF, Vancouver.



contents

- Introduction and motivation
- The optimization protocol
- Selected many-body results
- Expanded objective function
- Uncorrelated uncertainties
- Conclusions

Introduction

Any “potential model” will contain coupling constants that need to be determined from data one way or the other.

$$\min_{\vec{x}} \left[f(\vec{x}) = \sum_{q=1}^N \left(\frac{O(\vec{x})_q - O_q^{\text{exp}}}{w_q} \right)^2 \right]$$

Define an objective function that is relevant for the “objective”
“a well-founded and quantitative Hamiltonian for practical use”

Introduction

Any “potential model” will contain coupling constants that need to be determined from data one way or the other.

$$\min_{\vec{x}} \left[f(\vec{x}) = \sum_{q=1}^N \left(\frac{O(\vec{x})_q - O_q^{\text{exp}}}{w_q} \right)^2 \right]$$

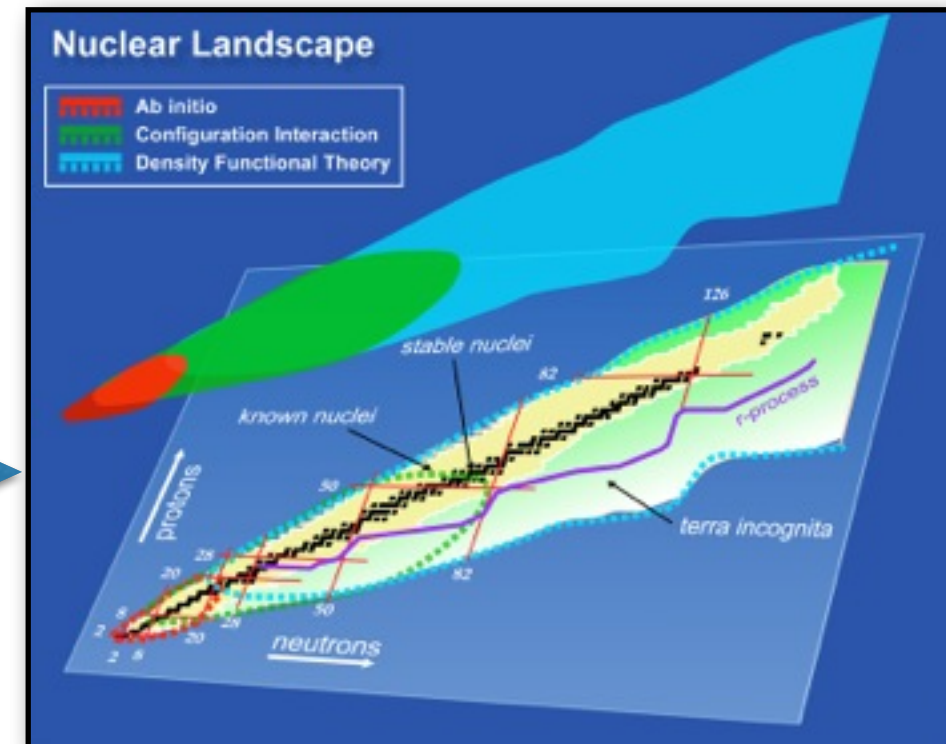
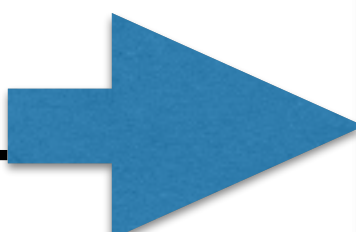
Define an objective function that is relevant for the “objective”
“a well-founded and quantitative Hamiltonian for practical use”

Several high-precision potentials on the market:

CD-Bonn, AV18, Idaho-N3LO, Nijmegen

Tlab (MeV)	N3LO (Idaho)	AV18
0-100	1.06	0.95
100-190	1.08	1.1
190-290	1.15	1.11
0-290	1.1	1.04

Chi Square



Chiral forces: current status

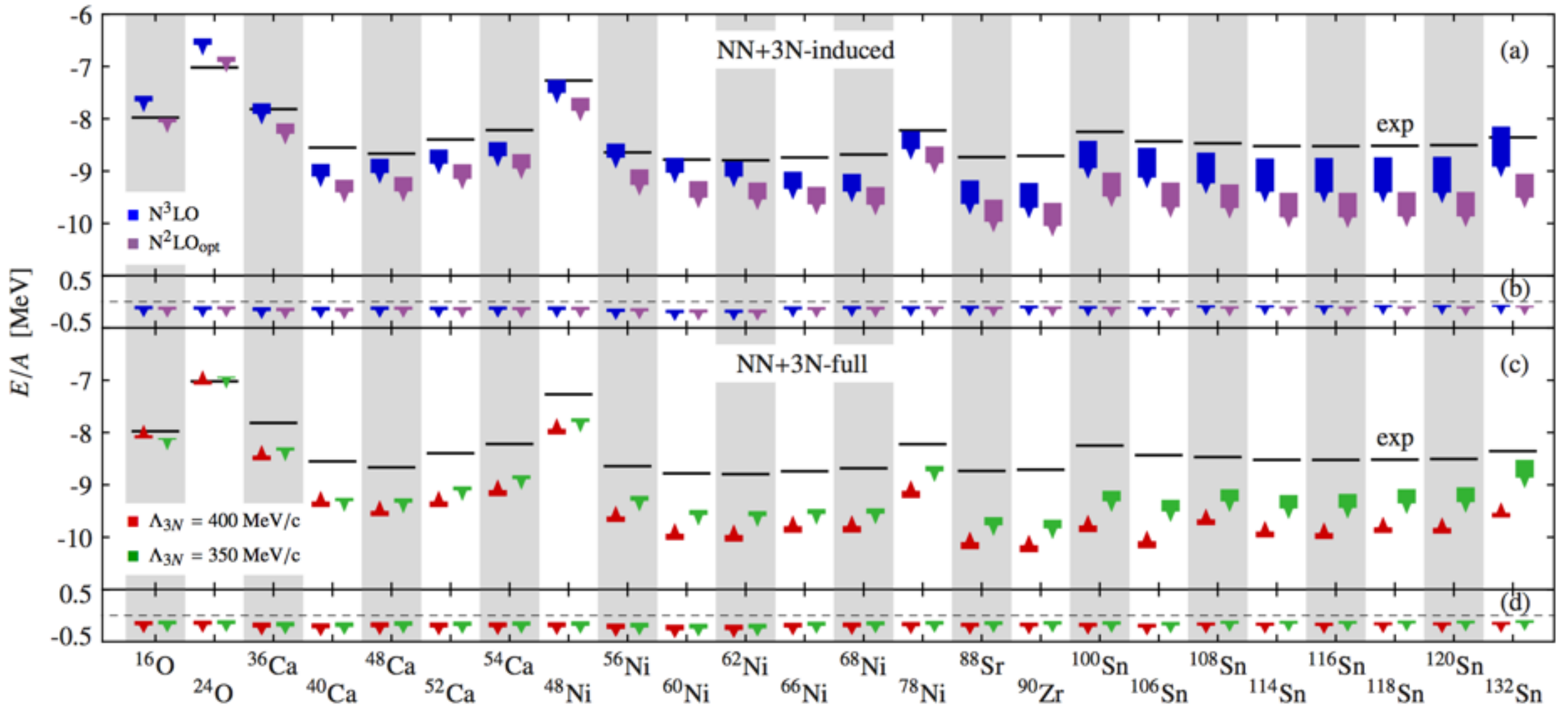


FIG. 5: (Color online) Ground-state energies from CR-CC(2,3) for (a) the $NN+3N$ -induced Hamiltonian starting from the $N^3\text{LO}$ and $N^2\text{LO}_{\text{opt}}$ NN interaction and (c) the $NN+3N$ -full Hamiltonian with $\Lambda_{3N} = 400 \text{ MeV}/c$ and $\Lambda_{3N} = 350 \text{ MeV}/c$. The boxes represent the spread of the results from $\alpha = 0.04 \text{ fm}^4$ to $\alpha = 0.08 \text{ fm}^4$, and the tip points into the direction of smaller values of α . Also shown are the contributions of the CR-CC(2,3) triples correction to the (b) $NN+3N$ -induced and (d) $NN+3N$ -full results. All results employ $\hbar\Omega = 24 \text{ MeV}$ and $3N$ interactions with $E_{3\max} = 18$ in NO2B approximation and full inclusion of the $3N$ interaction in CCSD up to $E_{3\max} = 12$. Experimental binding energies [32] are shown as black bars.

**Chiral interactions are qualitatively OK, but systematically overbinds and generates too small charge radii.
The discrepancies increase with mass number.**

Current Work: Expanded objective function

$$\min_{\vec{x}} \left[f(\vec{x}) = \sum_d \frac{1}{w_d} \sum_q \left(\frac{O(\vec{x})_{d,q} - O_{d,q}^{\text{exp}}}{w_q} \right)^2 \right]$$

Terms included in the objective function

potential: $NN + 3NF$ (local or non-local) at NNLO

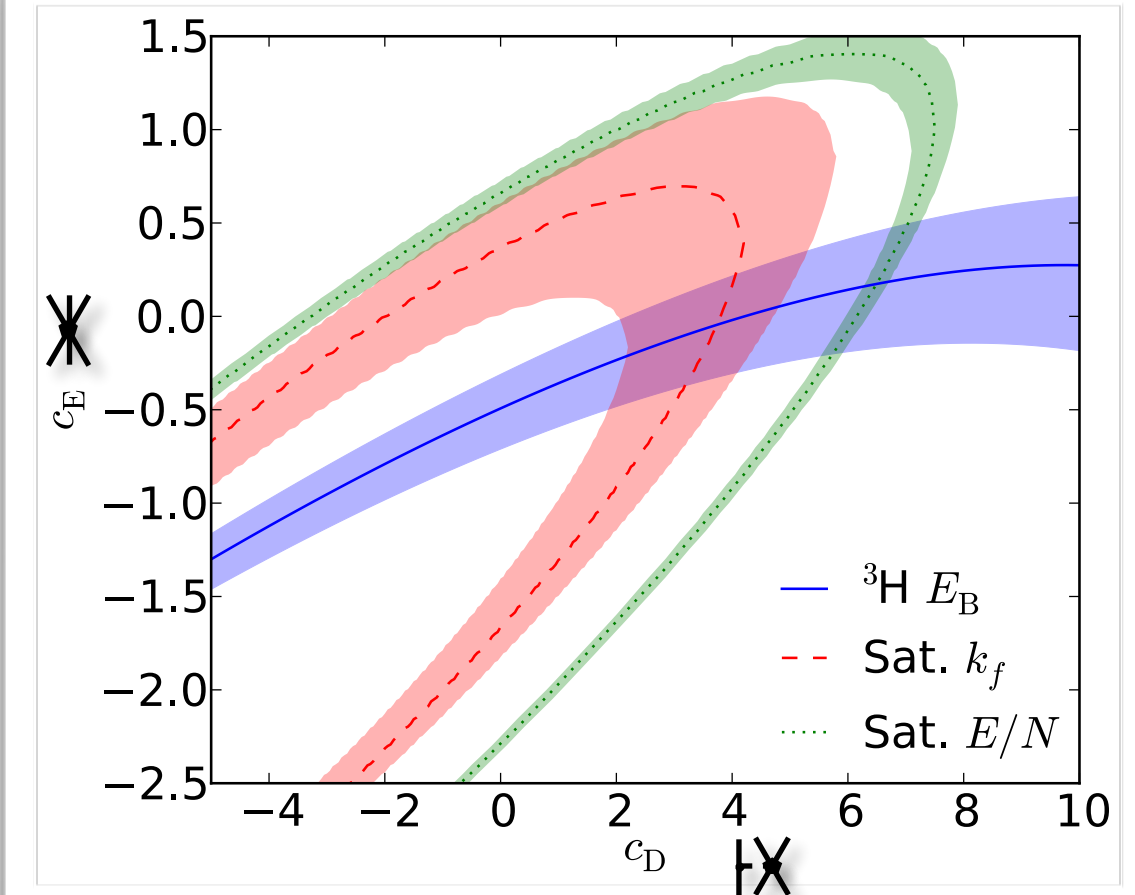
Nucleon-Nucleon scattering data

1S0 effective range expansion

Pion-Nucleon scattering phase shifts

Few-body observables:
NCSM 2H/3H/4He Binding energies and radii

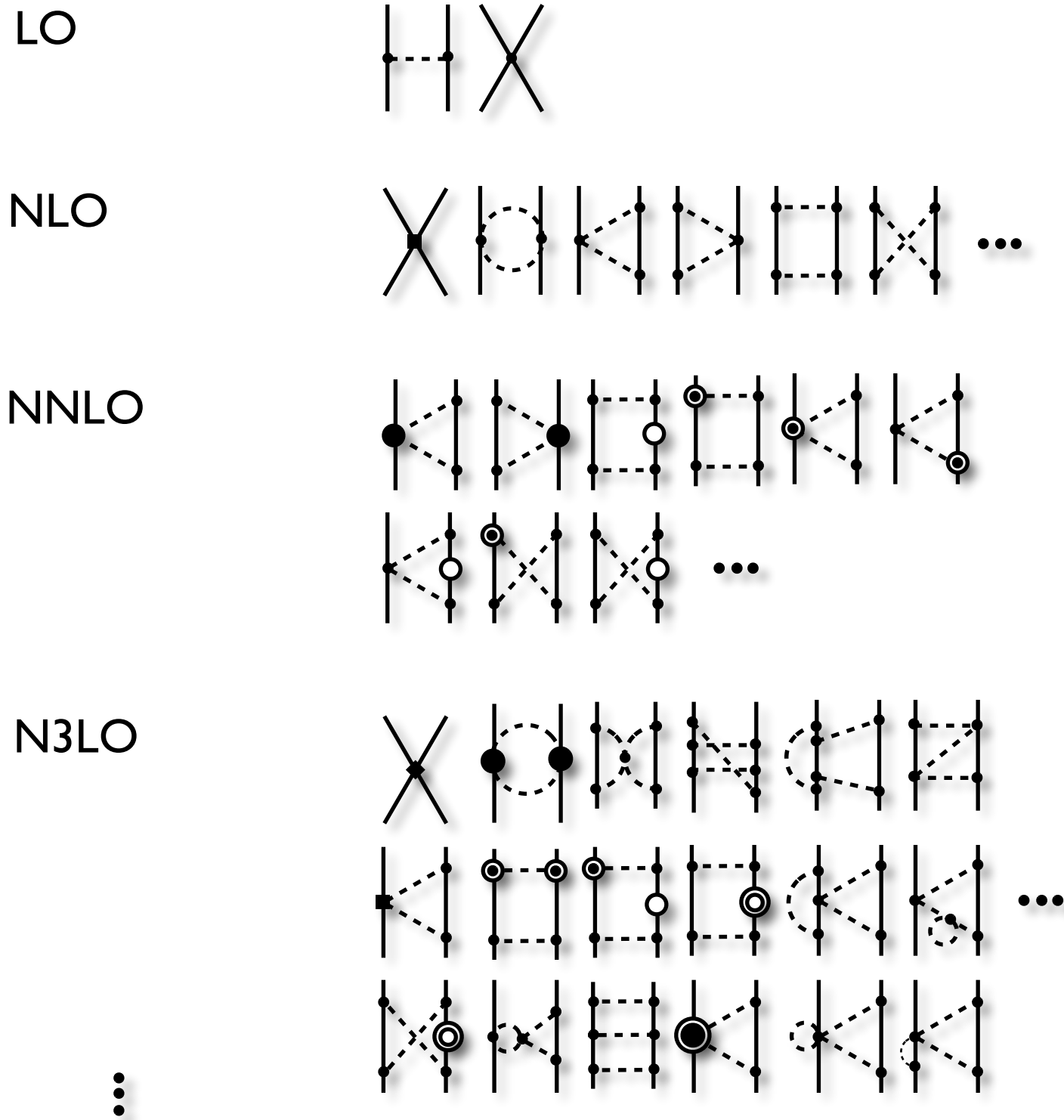
Energy and saturation momentum
of symmetric nuclear matter from
MBPT2



Nuclear forces from chiral EFT

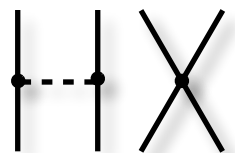
$$\begin{aligned}
\widehat{\mathcal{L}}^{\Delta=0} = & \frac{1}{2}\partial_\mu\pi\cdot\partial^\mu\pi - \frac{1}{2}m_\pi^2\pi^2 + \frac{1-4\alpha}{2f_\pi^2}(\pi\cdot\partial_\mu\pi)(\pi\cdot\partial^\mu\pi) - \frac{\alpha}{f_\pi^2}\pi^2\partial_\mu\pi\cdot\partial^\mu\pi + \frac{8\alpha-1}{8f_\pi^2}m_\pi^2\pi^4 \\
& + \bar{N} \left[i\partial_0 - \frac{g_A}{2f_\pi} \boldsymbol{\tau} \cdot (\vec{\sigma} \cdot \vec{\nabla})\pi - \frac{1}{4f_\pi^2} \boldsymbol{\tau} \cdot (\pi \times \partial_0\pi) \right] N \\
& + \bar{N} \left\{ \frac{g_A(4\alpha-1)}{4f_\pi^3} (\boldsymbol{\tau} \cdot \pi) \left[\pi \cdot (\vec{\sigma} \cdot \vec{\nabla})\pi \right] + \frac{g_A\alpha}{2f_\pi^3} \pi^2 \left[\boldsymbol{\tau} \cdot (\vec{\sigma} \cdot \vec{\nabla})\pi \right] \right\} N \\
& - \frac{1}{2}C_S\bar{N}N\bar{N}N - \frac{1}{2}C_T(\bar{N}\vec{\sigma}N)\cdot(\bar{N}\vec{\sigma}N) + \dots, \\
\widehat{\mathcal{L}}^{\Delta=1} = & \bar{N} \left\{ \frac{\vec{\nabla}^2}{2M_N} - \frac{ig_A}{4M_Nf_\pi} \boldsymbol{\tau} \cdot \left[\vec{\sigma} \cdot \left(\overset{\leftarrow}{\nabla} \partial_0\pi - \partial_0\pi \overset{\rightarrow}{\nabla} \right) \right] - \frac{i}{8M_Nf_\pi^2} \boldsymbol{\tau} \cdot \left[\overset{\leftarrow}{\nabla} \cdot (\pi \times \vec{\nabla}\pi) - (\pi \times \vec{\nabla}\pi) \cdot \overset{\rightarrow}{\nabla} \right] \right\} N \\
& + \bar{N} \left[4c_1m_\pi^2 - \frac{2c_1}{f_\pi^2} m_\pi^2 \pi^2 + \left(c_2 - \frac{g_A^2}{8M_N} \right) \frac{1}{f_\pi^2} (\partial_0\pi \cdot \partial_0\pi) \right. \\
& \left. + \frac{c_3}{f_\pi^2} (\partial_\mu\pi \cdot \partial^\mu\pi) - \left(c_4 + \frac{1}{4M_N} \right) \frac{1}{2f_\pi^2} \epsilon^{ijk} \epsilon^{abc} \sigma^i \tau^a (\partial^j \pi^b) (\partial^k \pi^c) \right] N \\
& - \frac{D}{4f_\pi} (\bar{N}N)\bar{N} \left[\boldsymbol{\tau} \cdot (\vec{\sigma} \cdot \vec{\nabla})\pi \right] N - \frac{1}{2}E(\bar{N}N)(\bar{N}\boldsymbol{\tau}N) \cdot (\bar{N}\boldsymbol{\tau}N) + \dots, \\
\widehat{\mathcal{L}}^{\Delta=2} = & \mathcal{L}_{\pi\pi}^{(4)} + \widehat{\mathcal{L}}_{\pi N}^{(3)} + \widehat{\mathcal{L}}_{NN}^{(2)} + \dots, \\
\widehat{\mathcal{L}}^{\Delta=4} = & \widehat{\mathcal{L}}_{NN}^{(4)} + \dots,
\end{aligned}$$

Nuclear forces from chiral EFT

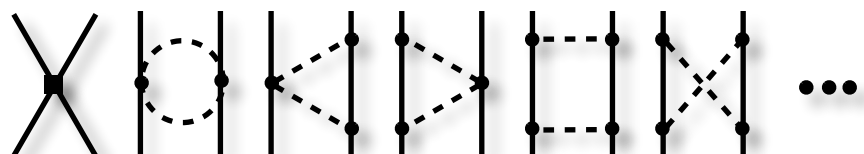


Nuclear forces from chiral EFT

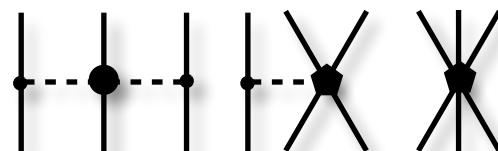
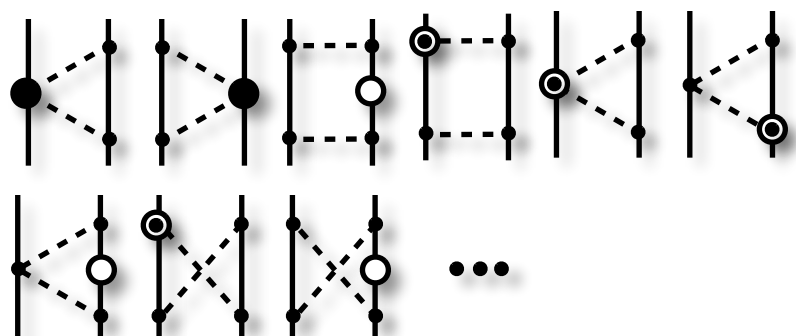
LO



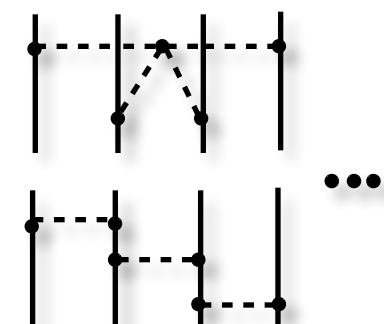
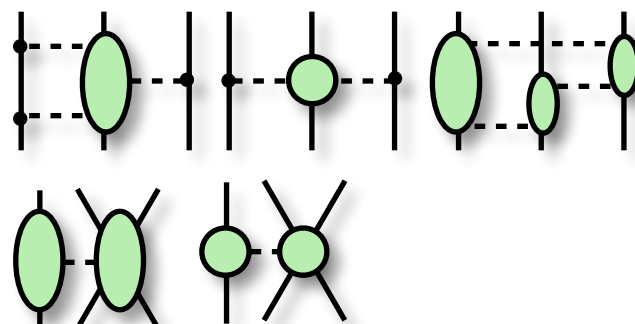
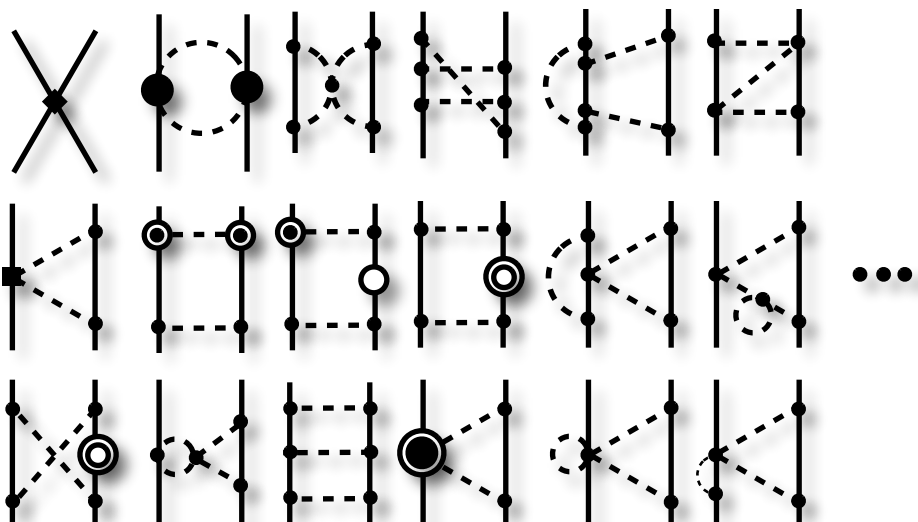
NLO



NNLO



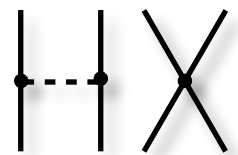
N3LO



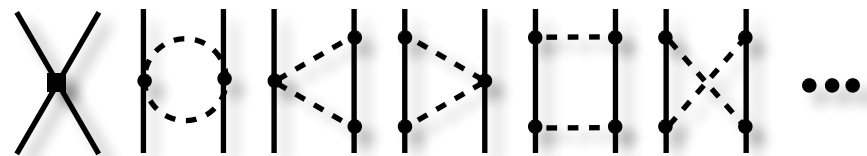
⋮

Nuclear forces from chiral EFT

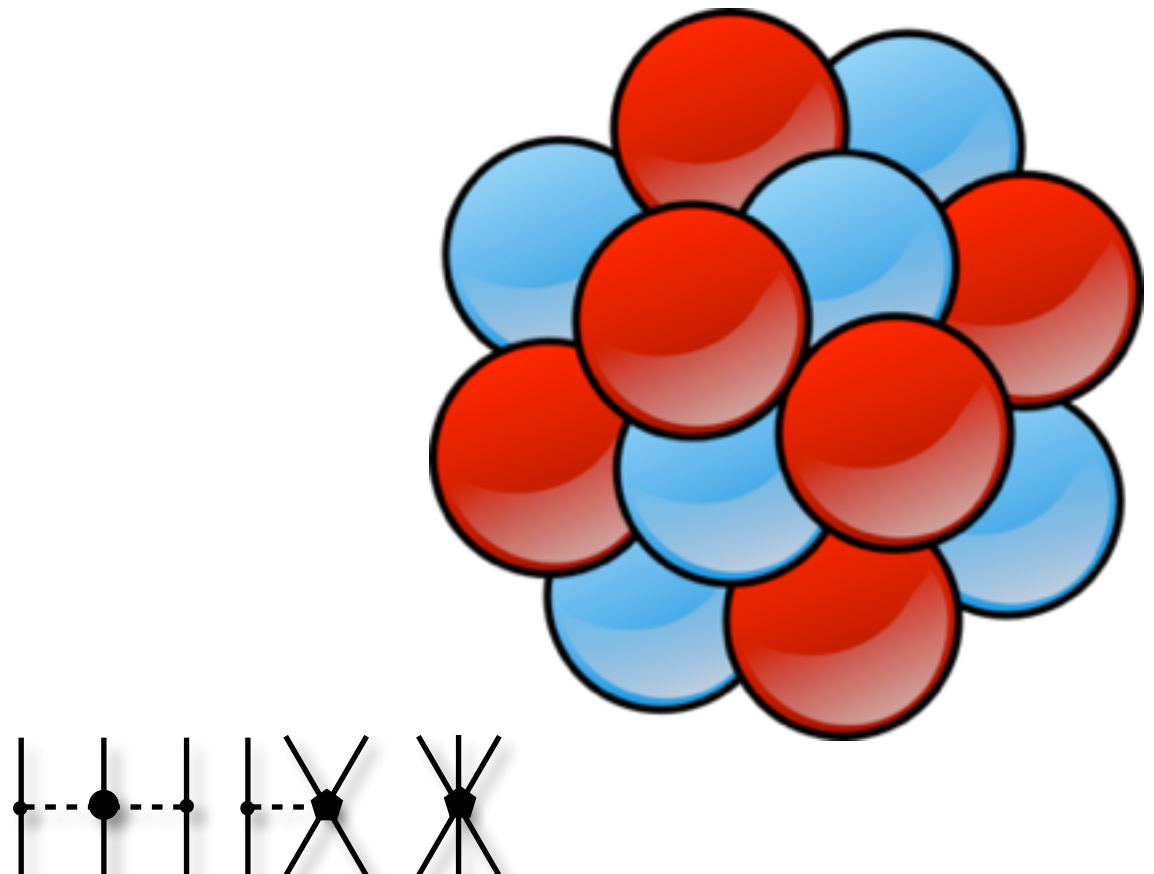
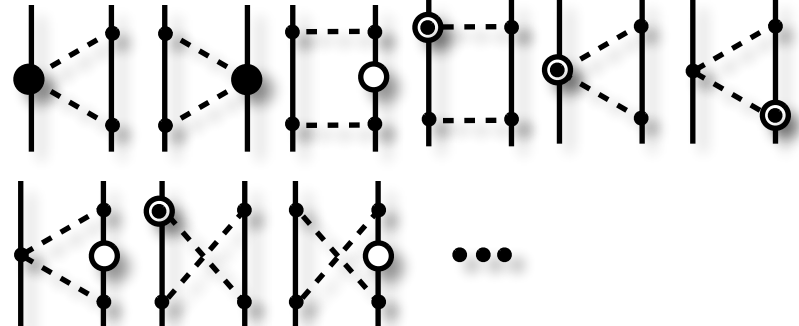
LO



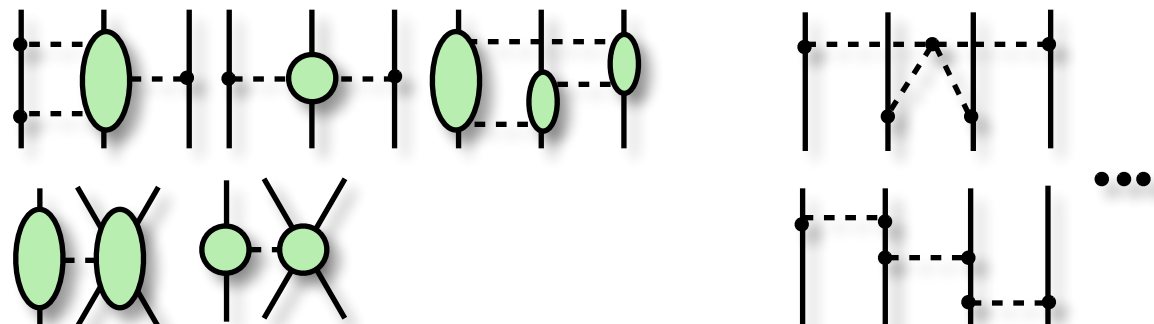
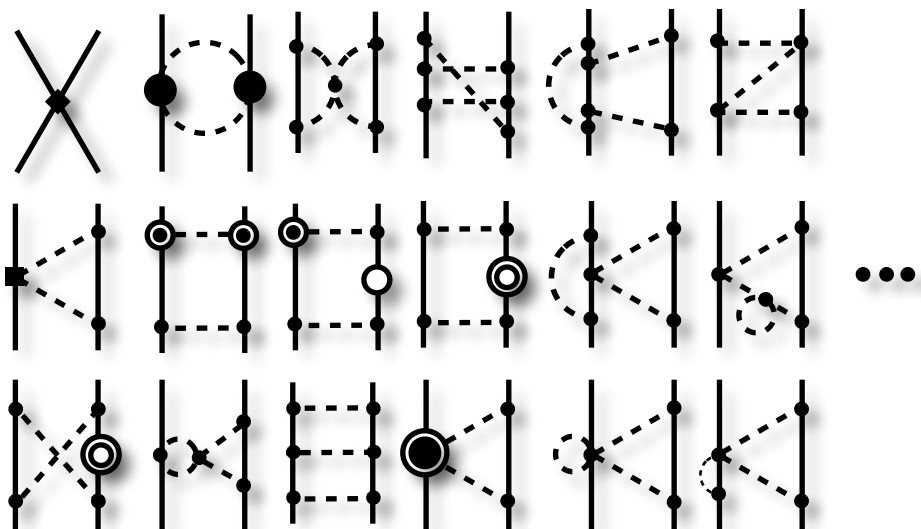
NLO



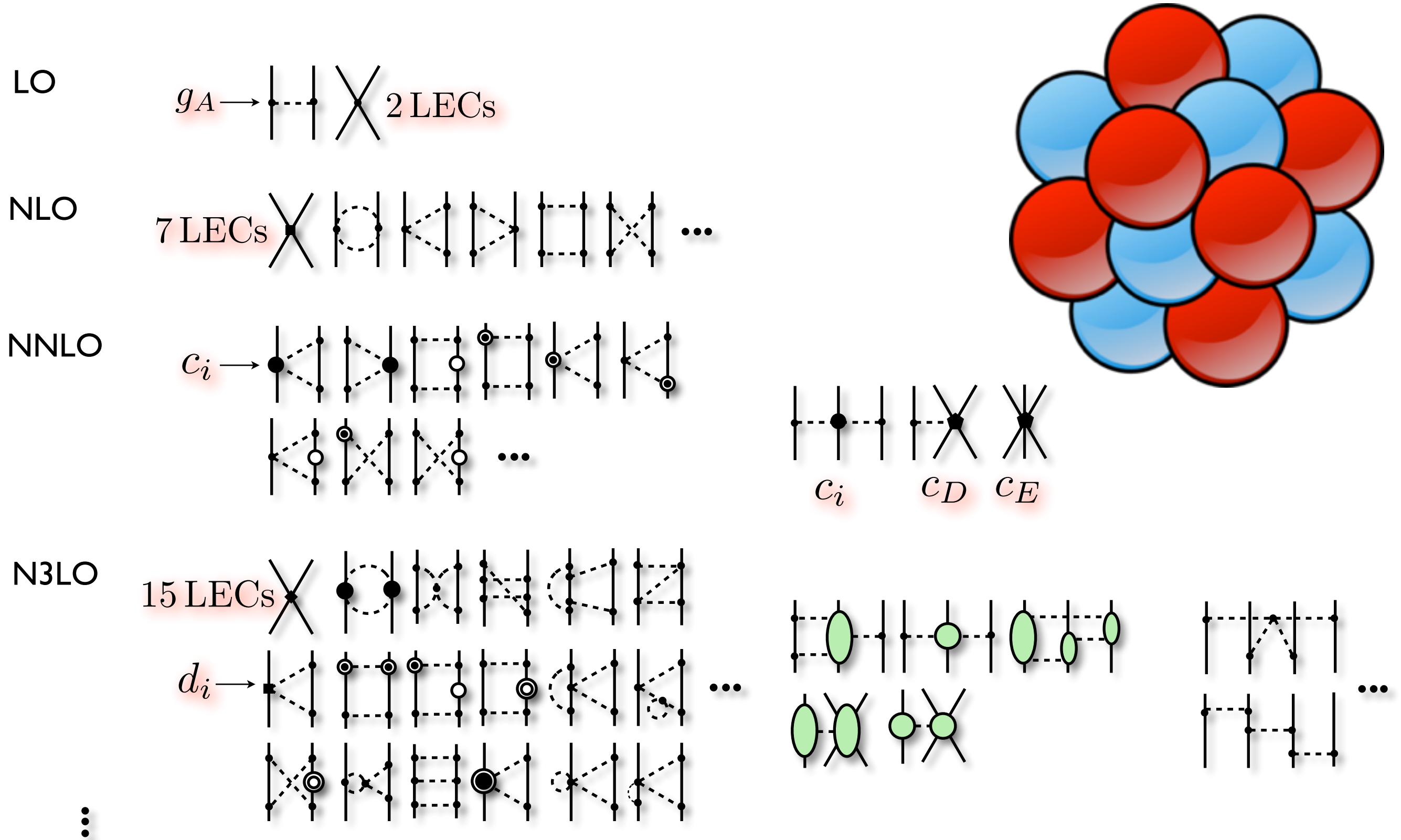
NNLO



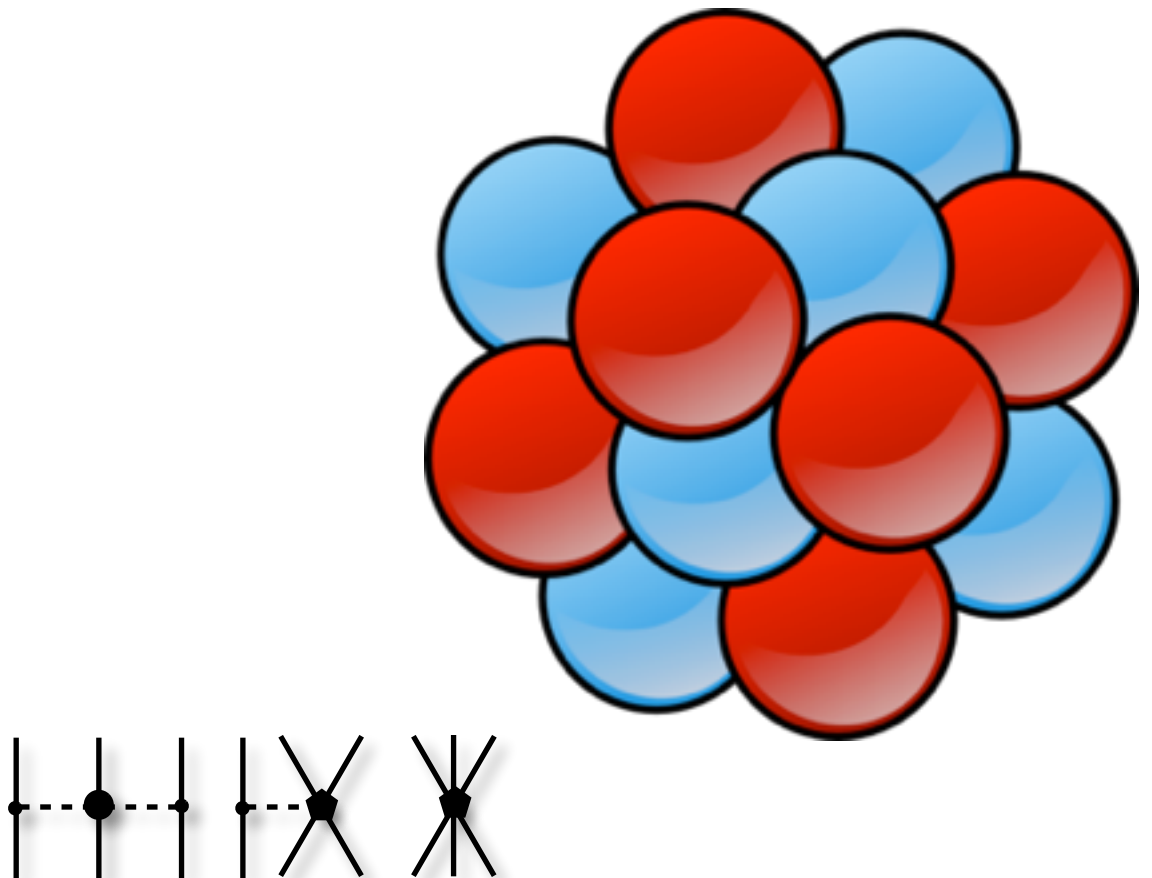
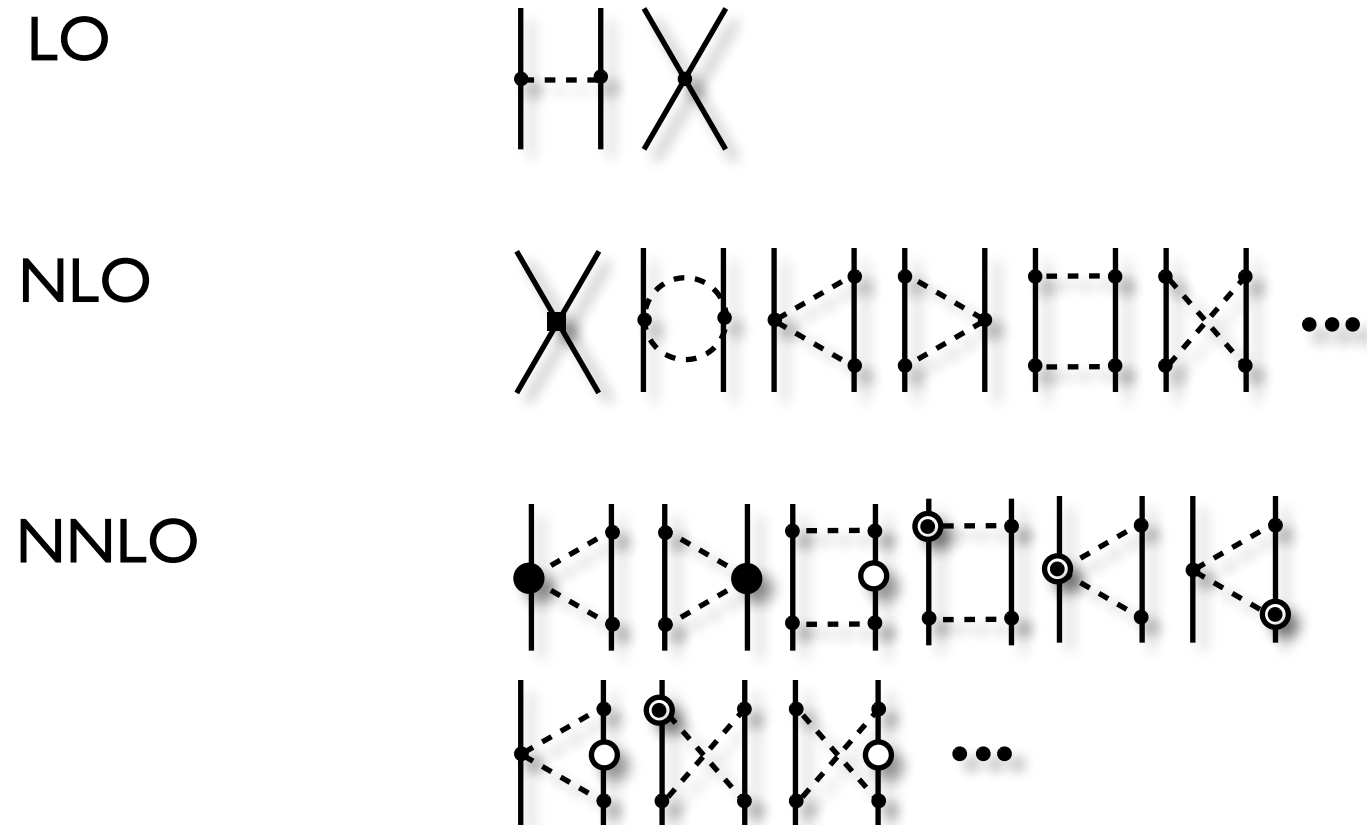
N3LO



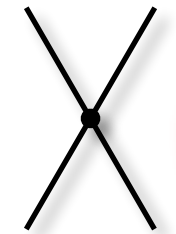
Nuclear forces from chiral EFT



Nuclear forces from chiral EFT

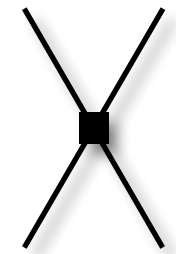


Low-energy constants at NNLO



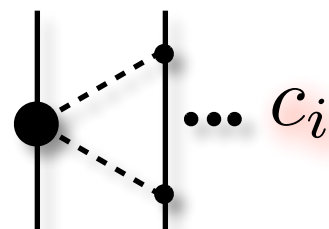
2 LECs

$$\tilde{C}_{^1S_0}^{pp} \tilde{C}_{^1S_0}^{np} \tilde{C}_{^1S_0}^{nn} \tilde{C}_{^3S_1}$$



7 LECs

$$C_{^1S_0} C_{^3P_0} C_{^3P_1} C_{^3P_2} \\ C_{^1P_1} C_{^3S_1} C_{^3S_1} - ^3D_1$$



c_i

$$c_1 \quad c_3 \quad c_4$$

long-range physics

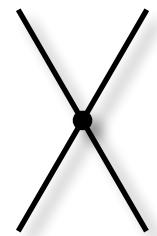
The contact potential

parametrizes the unresolved shortrange nuclear interaction.

In conventional meson theory, the short range force is described by heavy-meson exchange. The heavy mesons can't be resolved in ChPT.

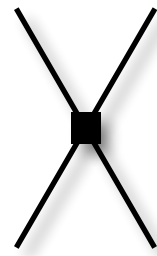
$$\frac{1}{m_\rho^2 + Q^2} \approx \frac{1}{m_\rho^2} \left(1 - \frac{Q^2}{m_\rho^2} + \frac{Q^4}{m_\rho^4} - \dots \right)$$

Low-energy constants at NNLO



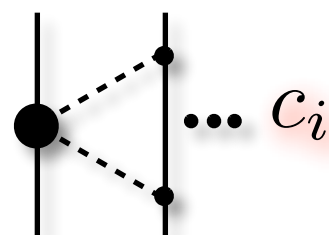
2 LECs

$$\tilde{C}_{^1S_0}^{pp} \tilde{C}_{^1S_0}^{np} \tilde{C}_{^1S_0}^{nn} \tilde{C}_{^3S_1}$$



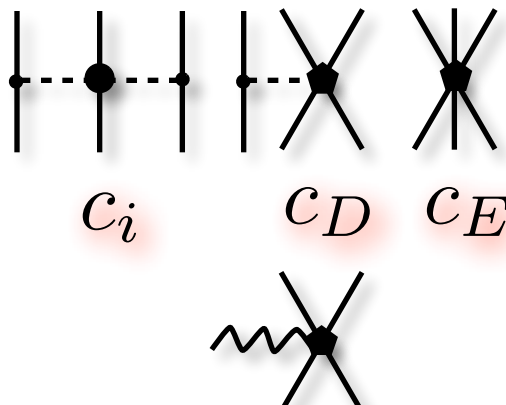
7 LECs

$$C_{^1S_0} C_{^3P_0} C_{^3P_1} C_{^3P_2} \\ C_{^1P_1} C_{^3S_1} C_{^3S_1} - ^3D_1$$



$$c_1 \quad c_3 \quad c_4$$

long-range physics



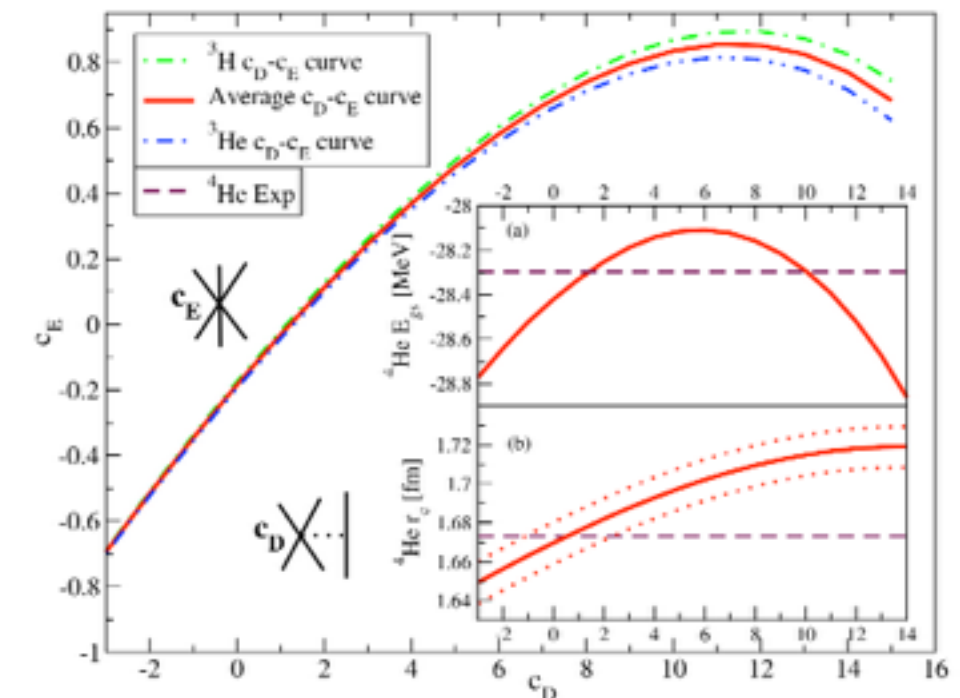
two new parameters that can be determined from the $A > 2$ systems

The contact potential

parametrizes the unresolved shortrange nuclear interaction.

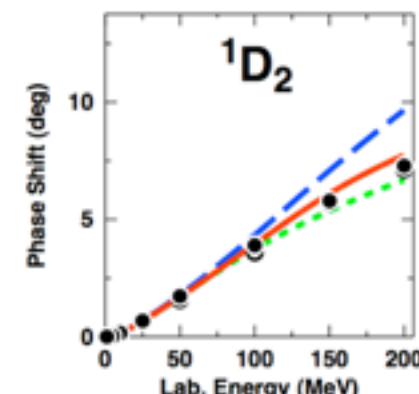
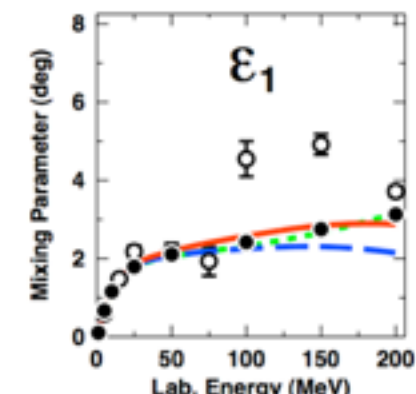
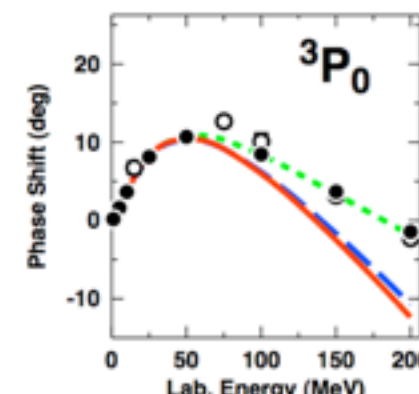
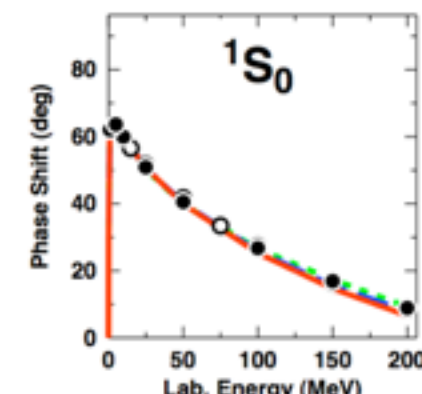
In conventional meson theory, the short range force is described by heavy-meson exchange. The heavy mesons can't be resolved in ChPT.

$$\frac{1}{m_{\rho^2+Q^2}} \approx \frac{1}{m_\rho^2} \left(1 - \frac{Q^2}{m_\rho^2} + \frac{Q^4}{m_\rho^4} - \dots \right)$$

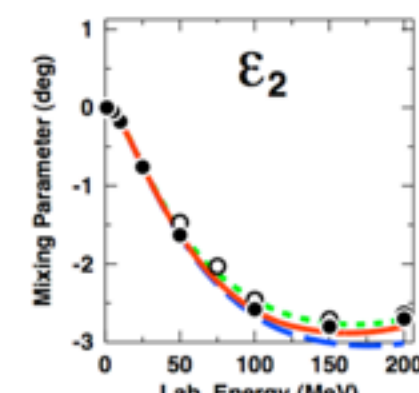
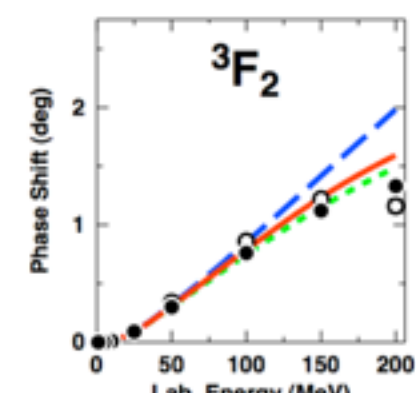
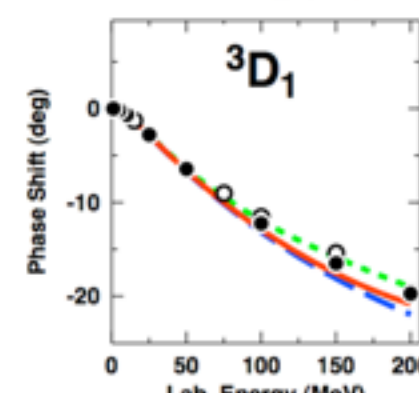
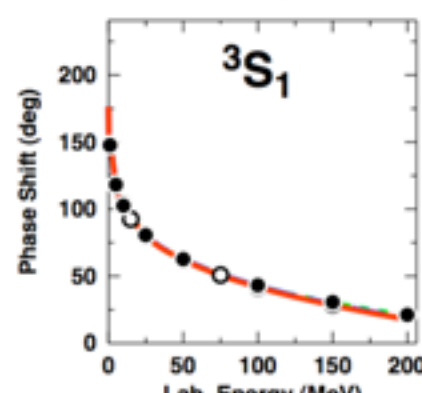
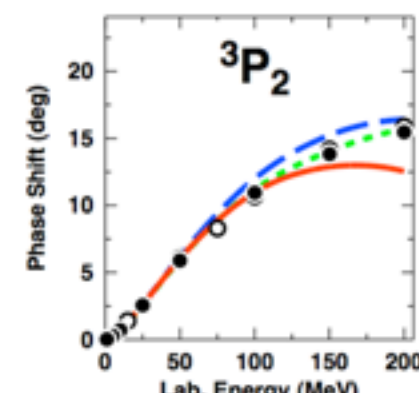
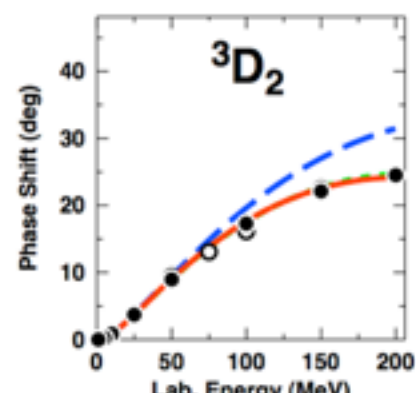
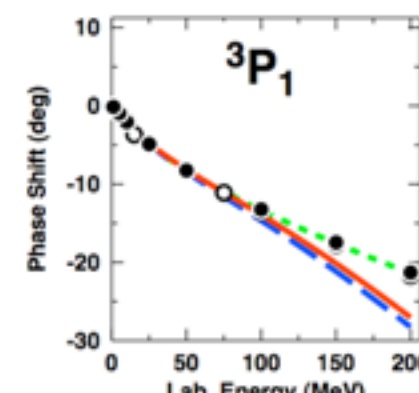
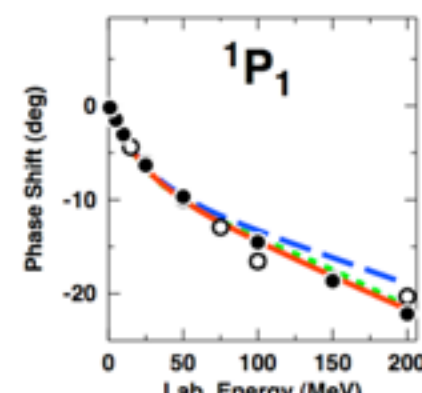


NNLOopt

T _{lab} (MeV)	NNLOopt(np)
0-35	0.85
35-125	1.17
125-183	1.87
183-290	6.09
0-290	2.95



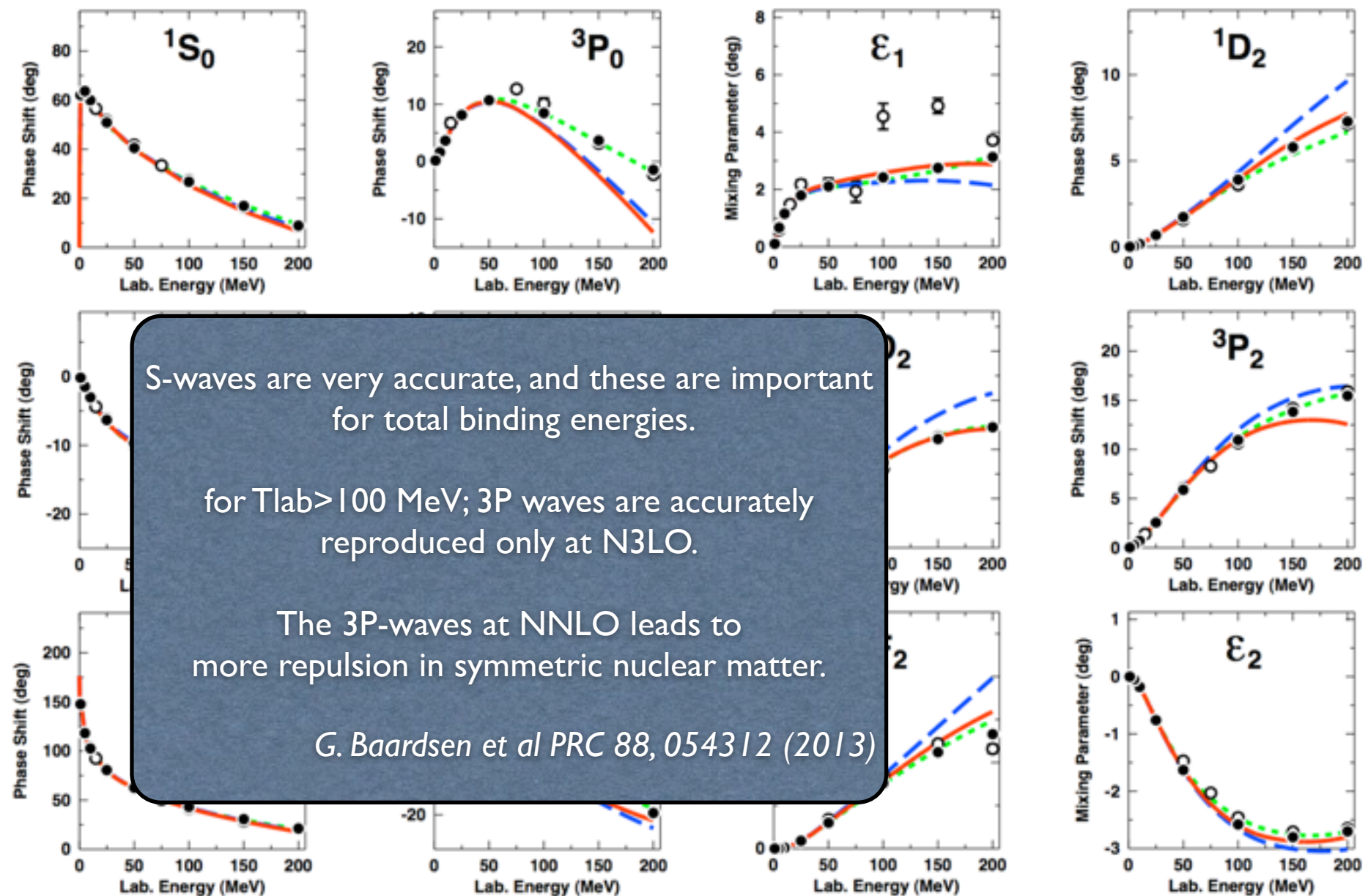
T _{lab} (MeV)	NNLOopt(pp)
0-35	1.11
35-125	1.56
125-183	23.95 (4.35)
183-290	29.26
0-290	17.10 (14.03)



Our first study, at next-to-next-to-leading order (NNLO), shows that there is room for improvement. Chi2 drops from $\sim 10-20$ to 3. Optimization has an impact on nuclear structure!

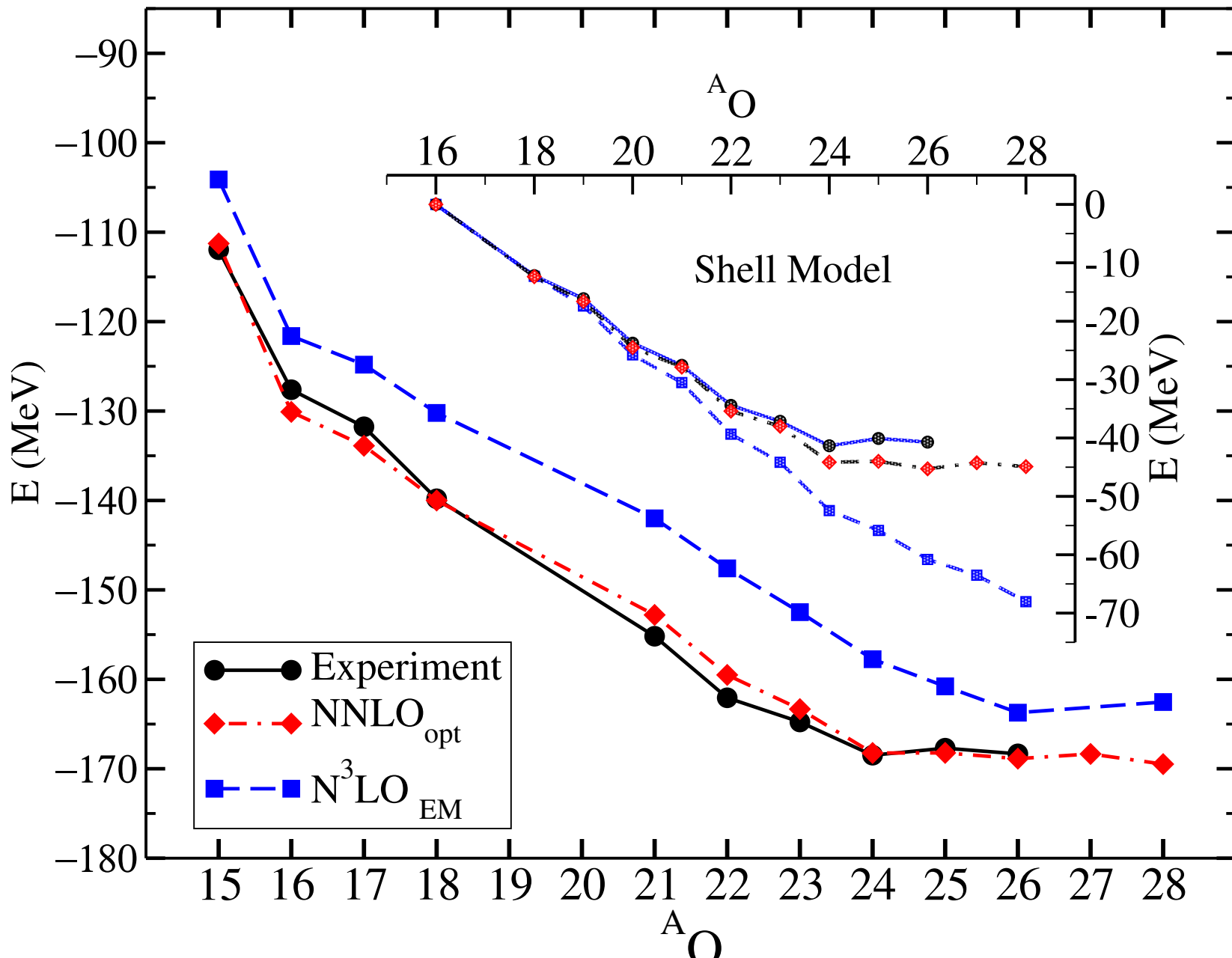
NNLOopt

T _{lab} (MeV)	NNLOopt(np)
0-35	0.85
35-125	1.17
125-183	1.87
183-290	6.09
0-290	2.95



Our first study, at next-to-next-to-leading order (NNLO), shows that there is room for improvement. Chi² drops from ~10-20 to 3. Optimization has an impact on nuclear structure!

Oxygen isotopes



1970: last stable
oxygen isotope 240

2012/2013: 26O unstable
(MSU, GSI, RIKEN)

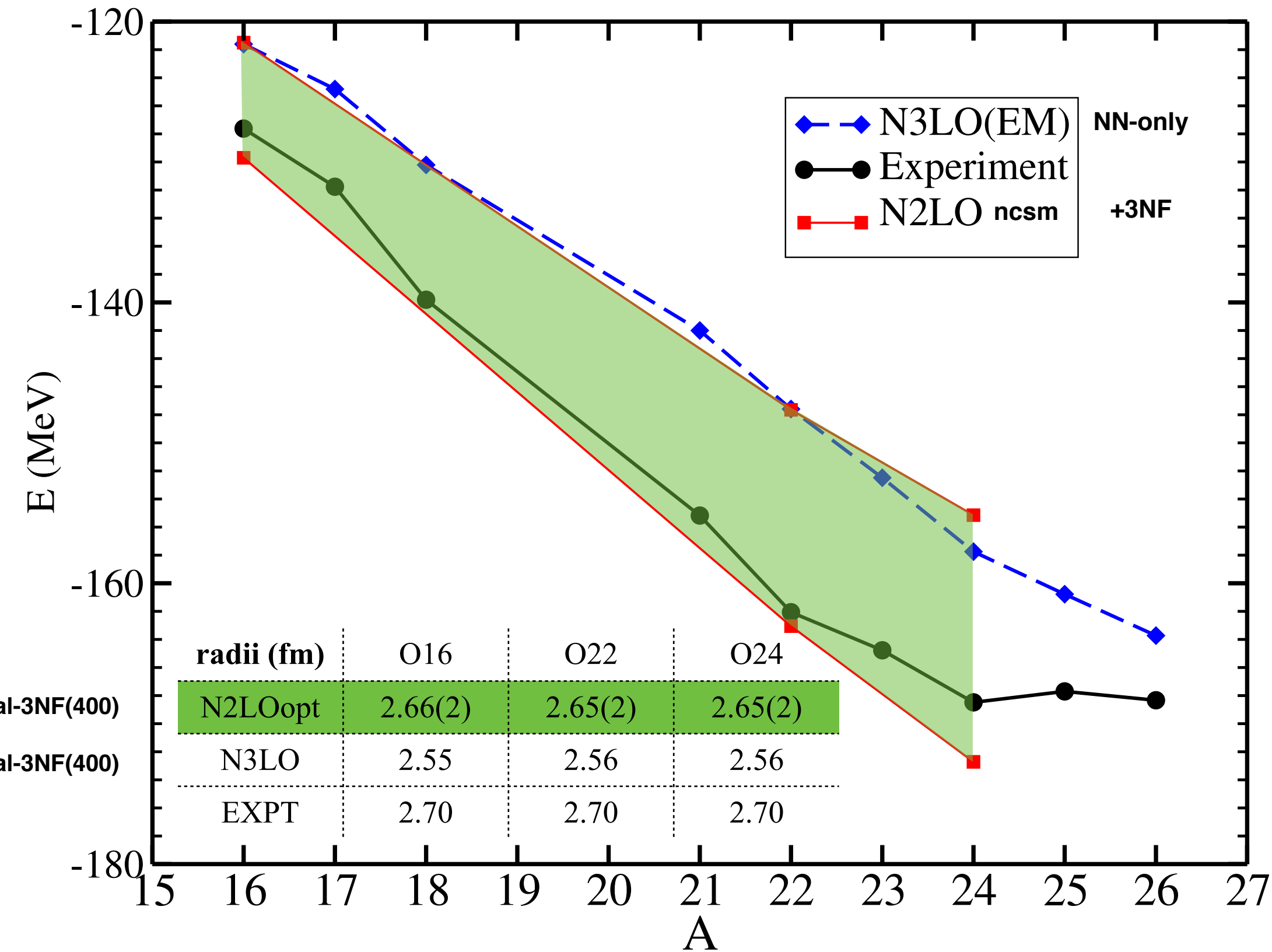
sd-shell model
effective interaction from
g-matrix and MBPT(3)
s.p.e. from exp ^{17}O spectrum.

Λ -CCSD(T), HF-basis
 $N_{\max}=15$ $\hbar\omega=20$ MeV

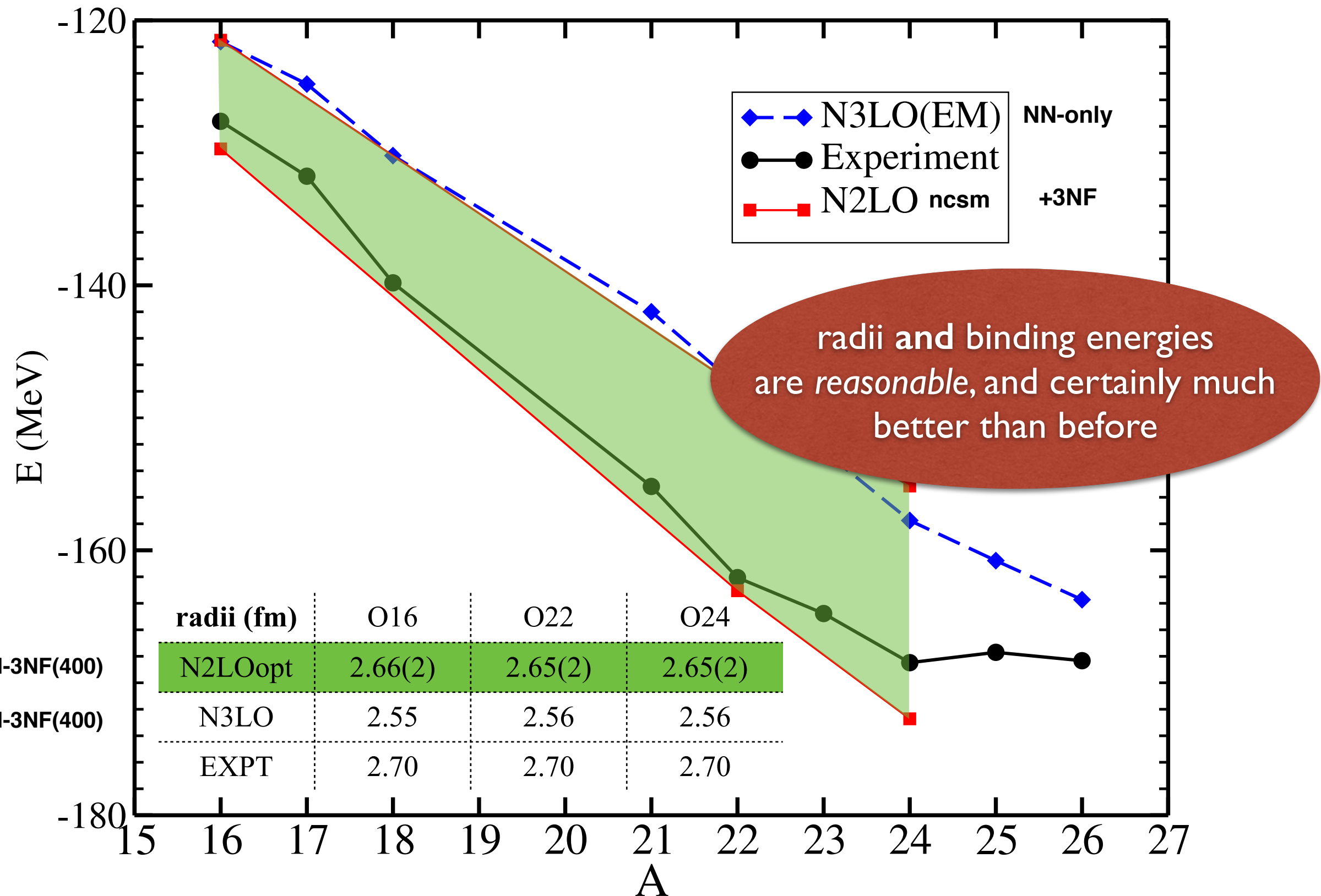
Oxygen dripline at $A=24$
with optimized 2-body force!

	^{16}O	^{22}O	^{24}O
NNLO _{opt}	-130.28	-159.76	-168.45
NNLO(EGM 450/500)	-156.76	-208.85	-225.65
Experiment	-127.62	-162.06	-168.48

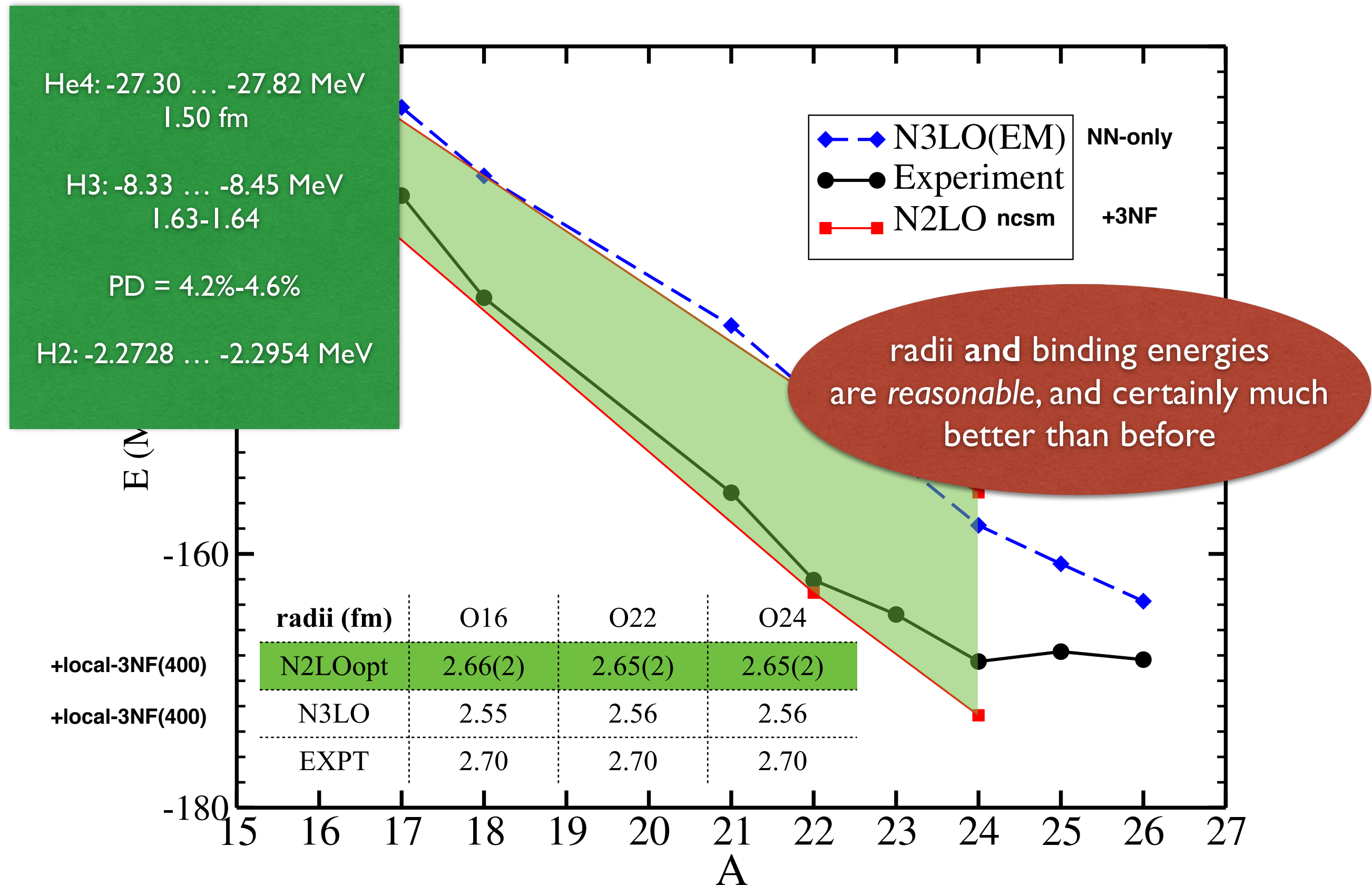
Preliminary: Oxygen from NCSM-objective function



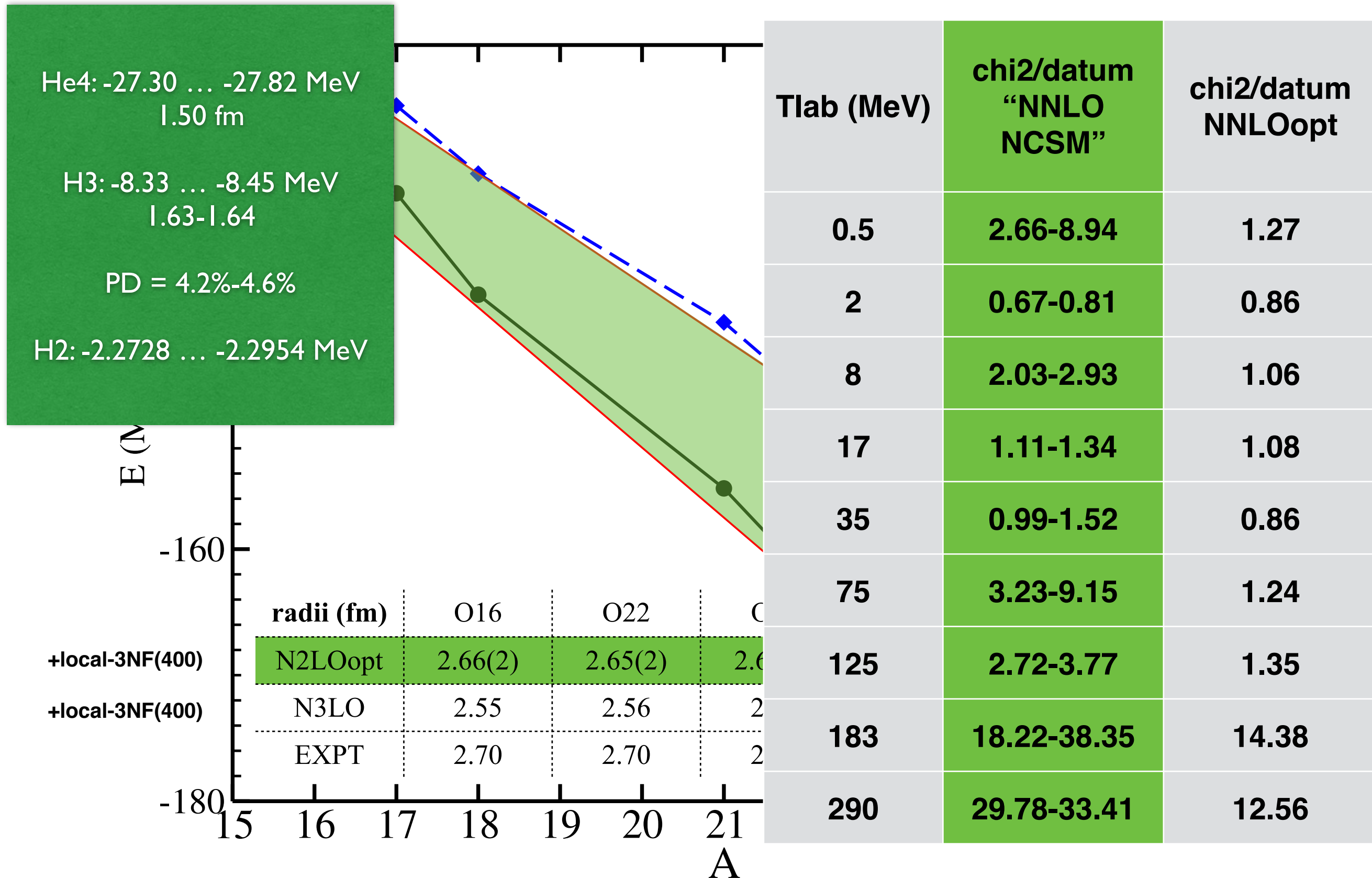
Preliminary: Oxygen from NCSM-objective function



Preliminary: Oxygen from NCSM-objective function



Preliminary: Oxygen from NCSM-objective function



πN LECs: overview

	piN-Krebs	piN-BM	NN-PWA	NNLO (Juelich)	N3LO (Idaho)	NNLOopt
c1	[-1.13,-0.75]	-0.81±0.12	-0.76±0.07	-0.81	-0.81	-0.9186
c3	[-5.51,-4.77]	-4.70±1.16	-4.78±0.10	-3.4	-3.2	-3.8887
c4	[3.34,3.71]	3.40±0.04	+3.96±0.22	+3.40	+5.40	+4.3103

piN-Krebs:

The most recently published, and to fourth order, analysis of the piN scattering phase shifts up to pLab=150 MeV [GW06,KH86]



1232 MeV

piN-BM:

Analysis of KA84 piN scattering phase shifts pLab=40-97

NN-PWA:

Nijmegen PWA analysis of NN scattering data, with the long range physics described by subleading chiral two-pion exchanges

NNLO (Juelich):

pion-nucleon couplings taken from piN-BM, but c3 chosen on the larger side within the uncertainty. This value is consistent with the Entem Machleidt analysis of NN data.

N3LO (Idaho):

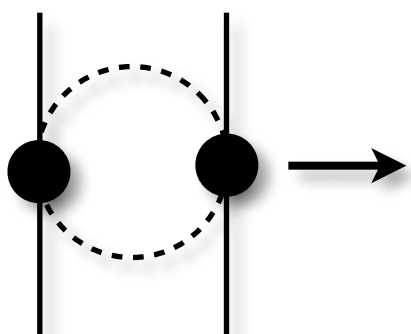
Guided by fit to NN data

NNLOopt:

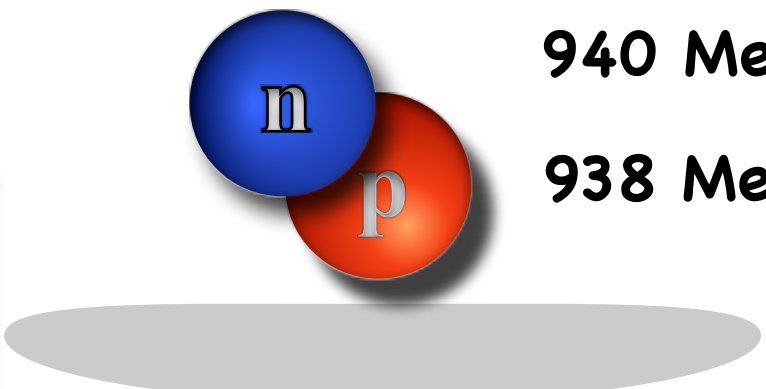
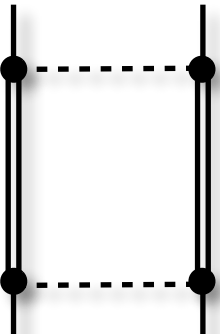
Guided by fit to NN data

resonance saturation

Δ-less



Δ-full



E. Epelbaum et al. Rev. Mod. Phys. 81, 1773 (2009)

E. Epelbaum et al. Eur. Phys. J. A19, 401 (2004)

R. Machleidt et al. Phys. Rep. 503, 1 (2011)

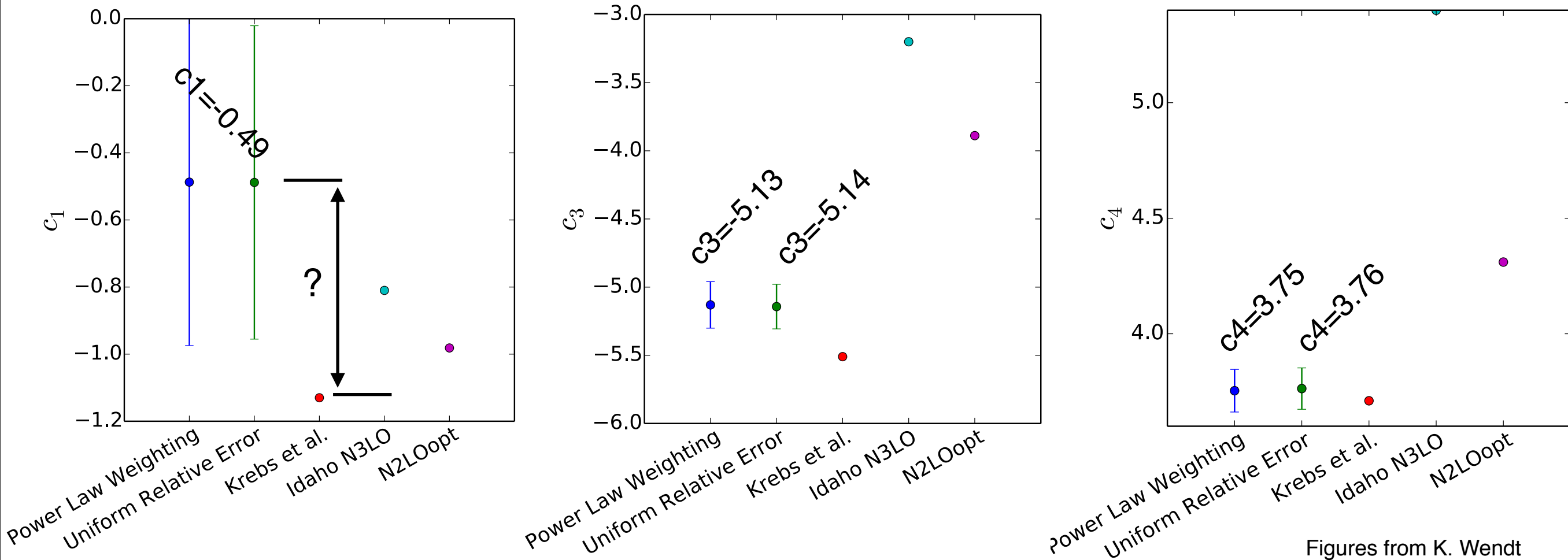
A. Ekström et al. Phys. Rev. Lett. 110, 192502 (2013)

H. Krebs et al. Phys. Rev. C 85, 054006 (2012)

M. C. M. Rentmeester et al. Phys. Rev. C, 67, 044001 (2003)

πN LECs: our results

	piN-Krebs	piN-BM	NN-PWA	NNLO (Juelich)	N3LO (Idaho)	NNLOopt
c1	[-1.13,-0.75]	-0.81±0.12	-0.76±0.07	-0.81	-0.81	-0.9186
c3	[-5.51,-4.77]	-4.70±1.16	-4.78±0.10	-3.4	-3.2	-3.8887
c4	[3.34,3.71]	3.40±0.04	+3.96±0.22	+3.40	+5.40	+4.3103



Figures from K. Wendt

πN LECs: our results

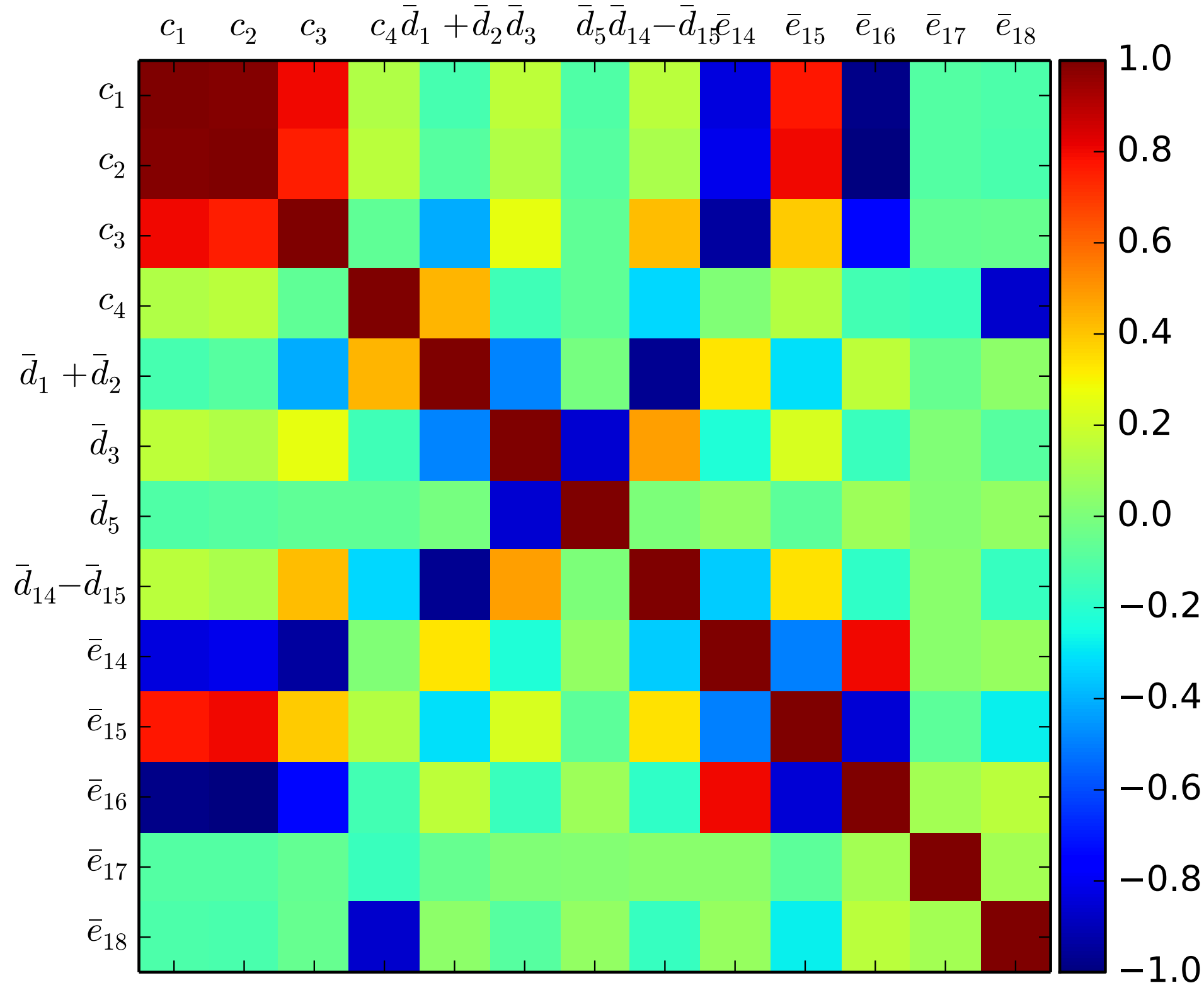


Figure from K. Wendt

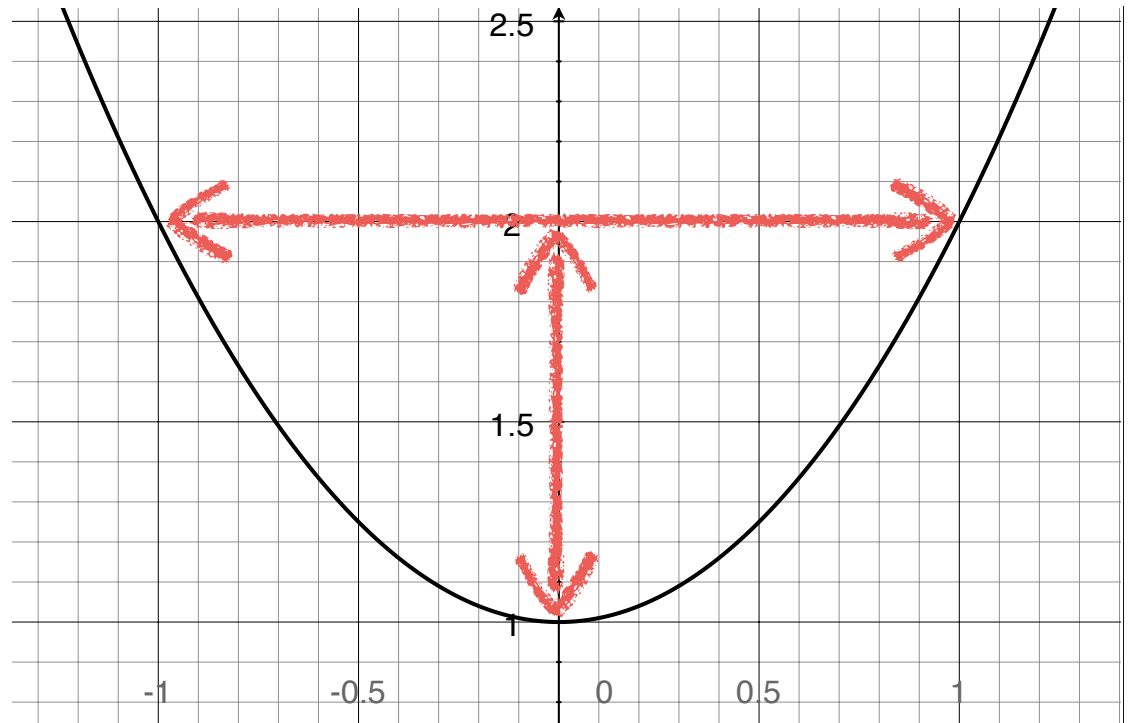
NNLOopt uncertainty estimates (ongoing)

SIMPLE ESTIMATES of the statistical uncertainties of the LECs that come from the experimental cross section errors.

Pros: fast and gives a first hint on the uncertainty and sensitivity of the potential with respect to variations in the parameter values

Cons: neglects all parameter correlations.

(Only OK in the gaussian limit, i.e. where the chi2 curve is parabolic)



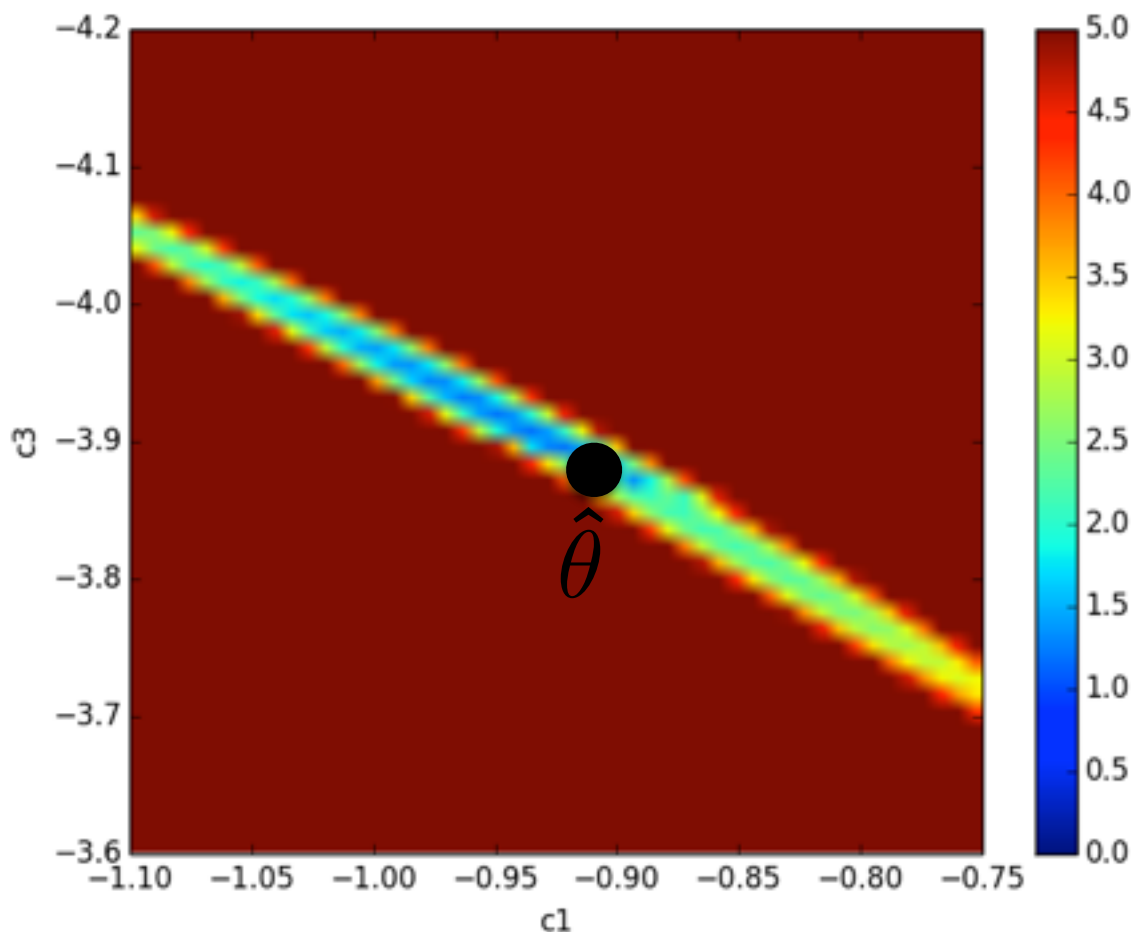
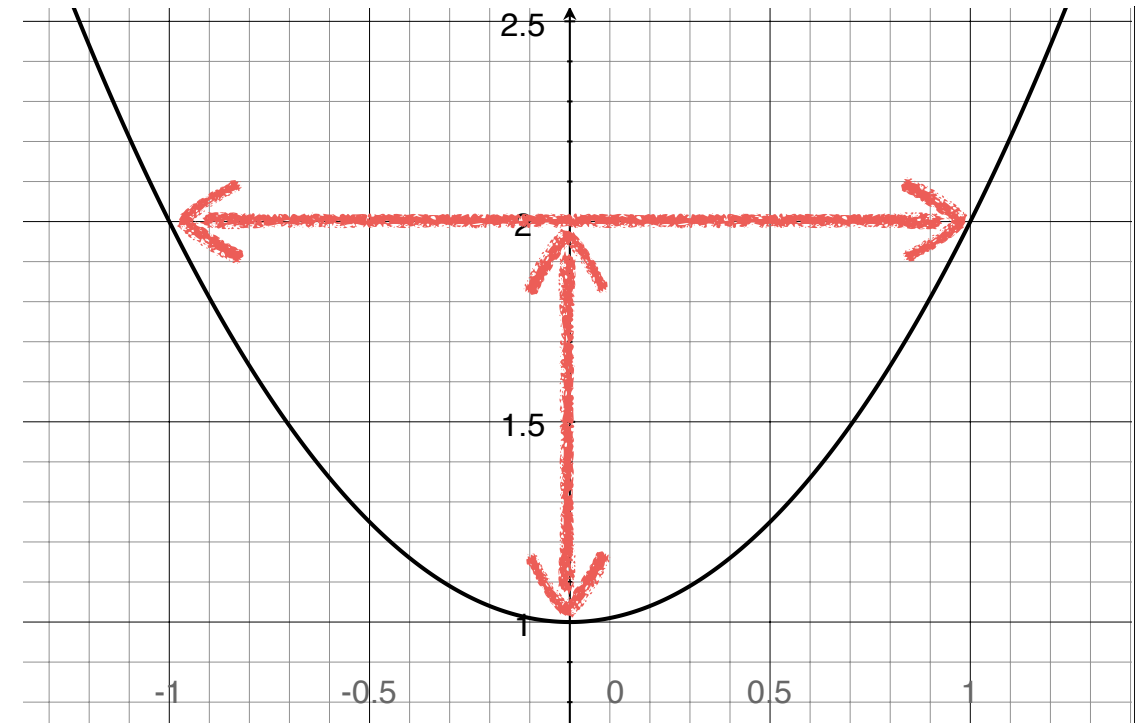
NNLOopt uncertainty estimates (ongoing)

SIMPLE ESTIMATES of the statistical uncertainties of the LECs that come from the experimental cross section errors.

Pros: fast and gives a first hint on the uncertainty and sensitivity of the potential with respect to variations in the parameter values

Cons: neglects all parameter correlations.

(Only OK in the gaussian limit, i.e. where the chi2 curve is parabolic)



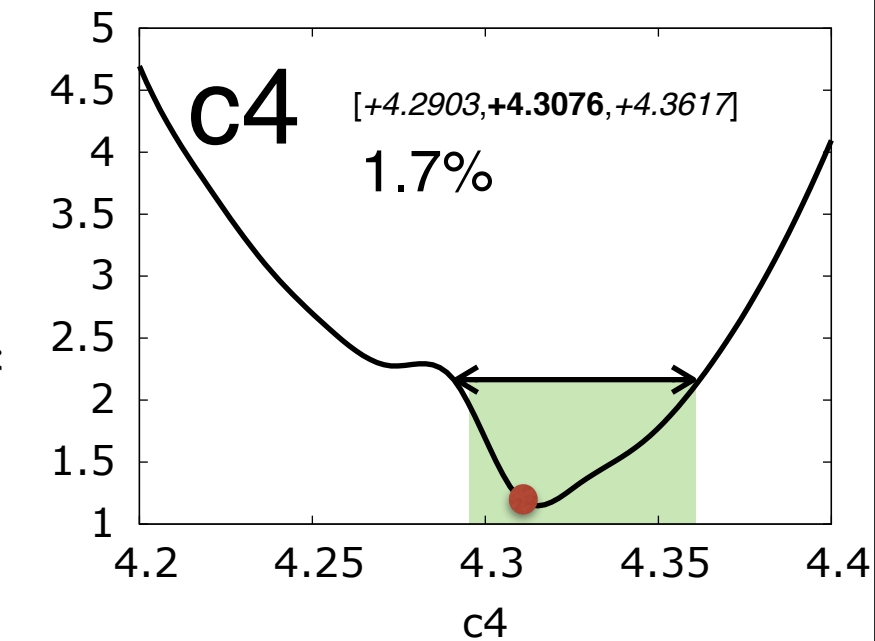
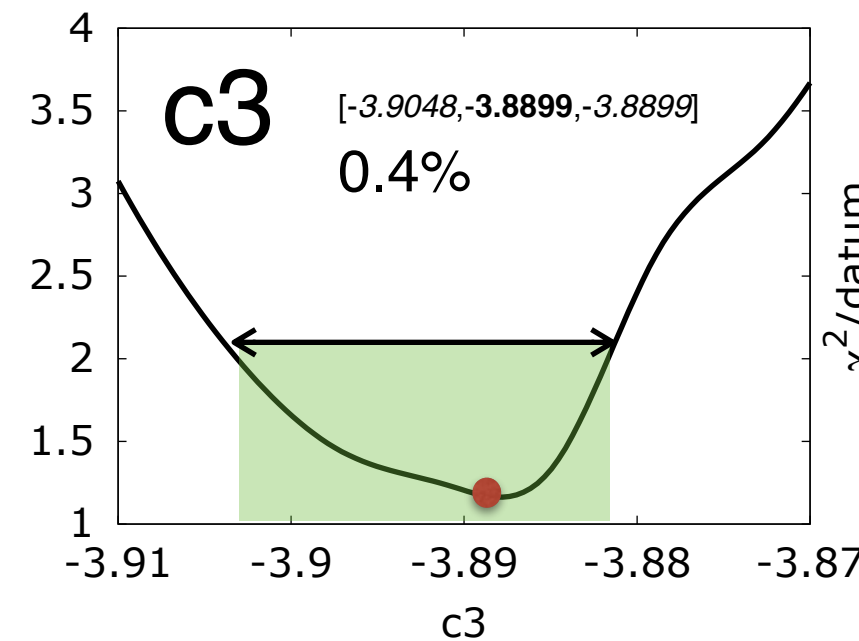
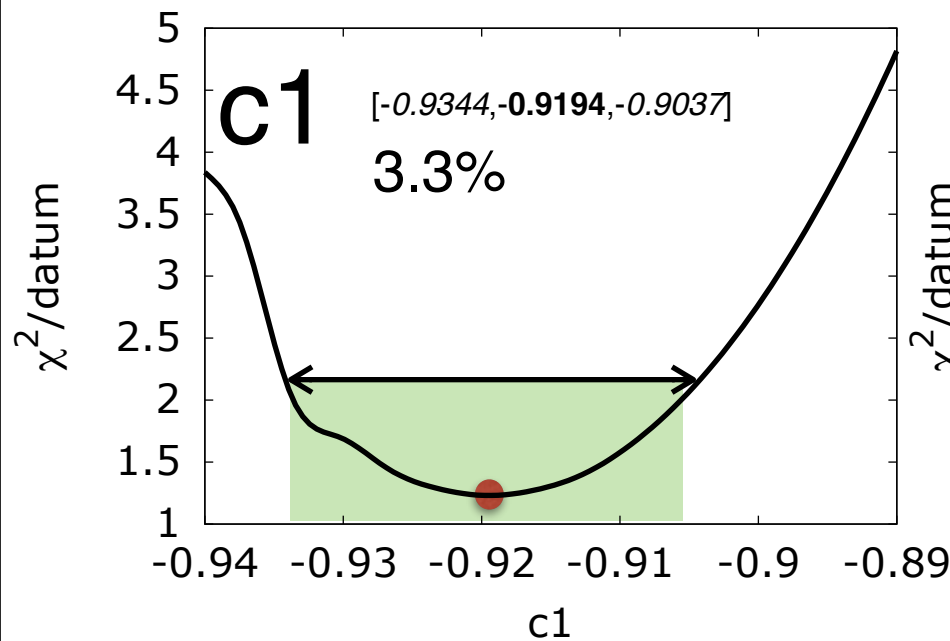
Compute Hessian of Chi2

$$\min_{\vec{x}} [f(\vec{x}) = \sum_d \sum_q \left(\frac{O(\vec{x})_{d,q} - O_{d,q}^{\text{exp}}}{w_q} \right)^2]$$

$$\text{cov}(p_i, p_j) \approx \frac{\chi^2}{N} H(\hat{\theta})^{-1}$$

Janet R. Donaldson and Robert B. Schnabel,
Technometrics, February 1987, Vol. 29, No. 1

NNLOopt (Tlab<125) uncertainty estimates

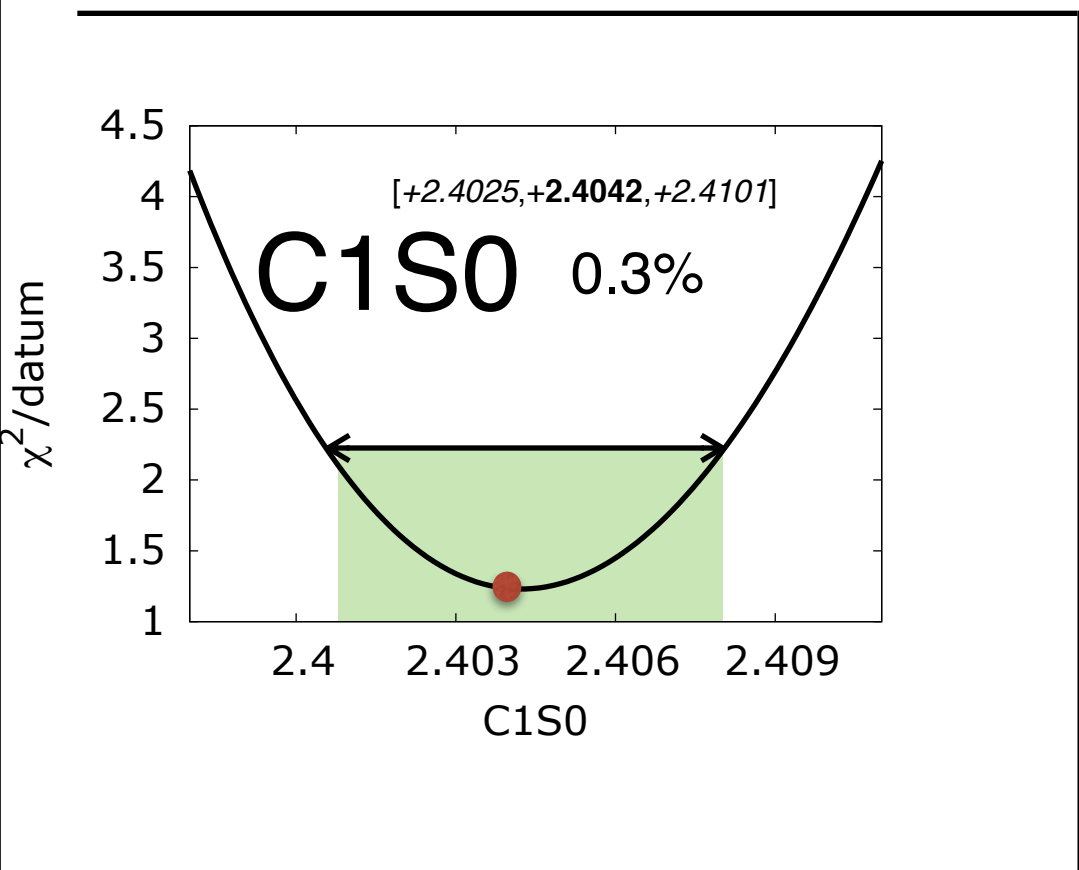
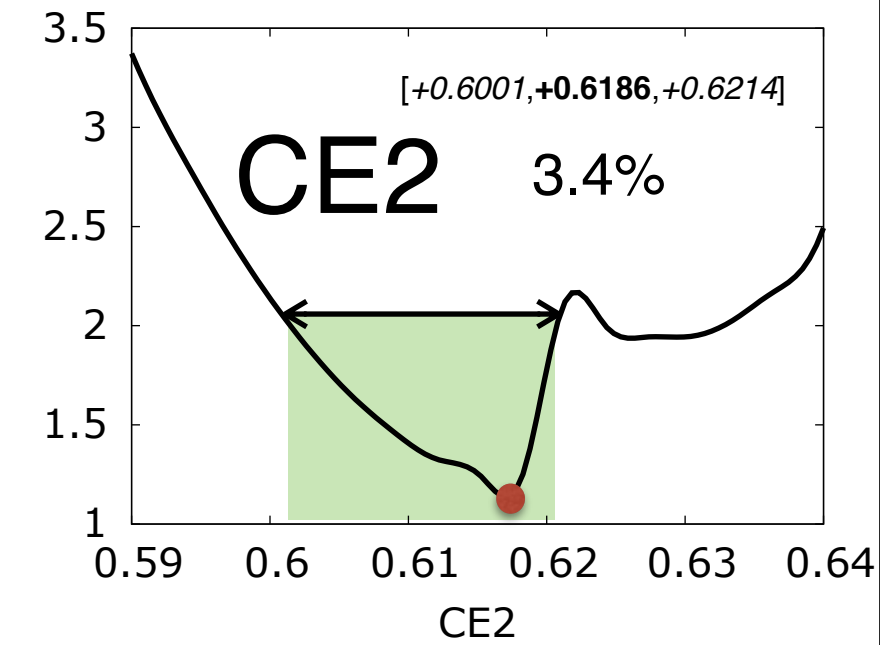
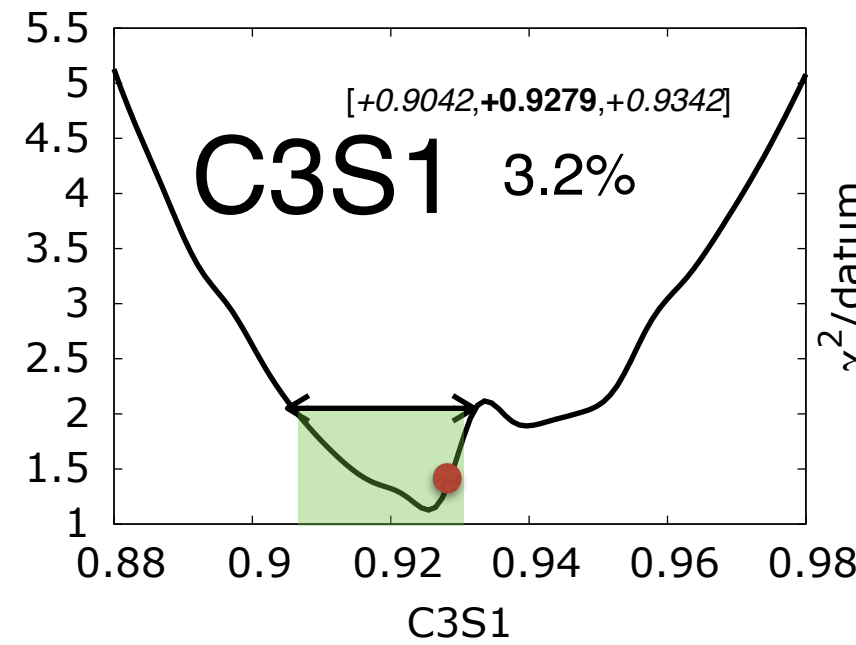
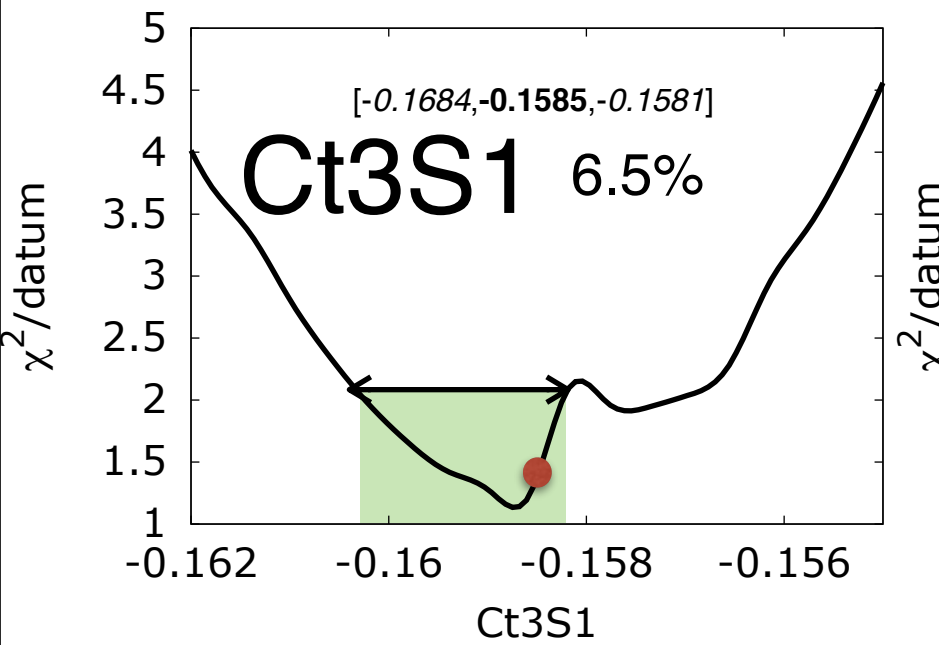


POTENTIAL: NNLOopt, further optimized wrt scattering data below Tlab=125.0 MeV

par.c1	= -0.9194168473672011
par.c3	= -3.8898982574932761
par.c4	= 4.3075828920511565
par.Ct_1S0np	= -0.1521600767237906
par.Ct_1S0pp	= -0.1513601095572962
par.Ct_3S1	= -0.1584760219635368
par.C_1S0	= 2.4042363751110987
par.C_3P0	= 1.2657410632596040
par.C_1P1	= 0.4147958250829769
par.C_3P1	= -0.7799477809574415
par.C_3S1	= 0.9278867972024134
par.C_3S1-3D1	= 0.6185795556481742
par.C_3P2	= -0.6735011268948335

```
#####
#          TOT          PP          NP
#  0.0    35.0   0.935777  1.020277  0.871546
#  35.0   125.0   1.429777  1.648994  1.272311
# 125.0   183.0   0.000000  0.000000  0.000000
# 183.0   290.0   0.000000  0.000000  0.000000
# 290.0   350.0   0.000000  0.000000  0.000000
#####
```

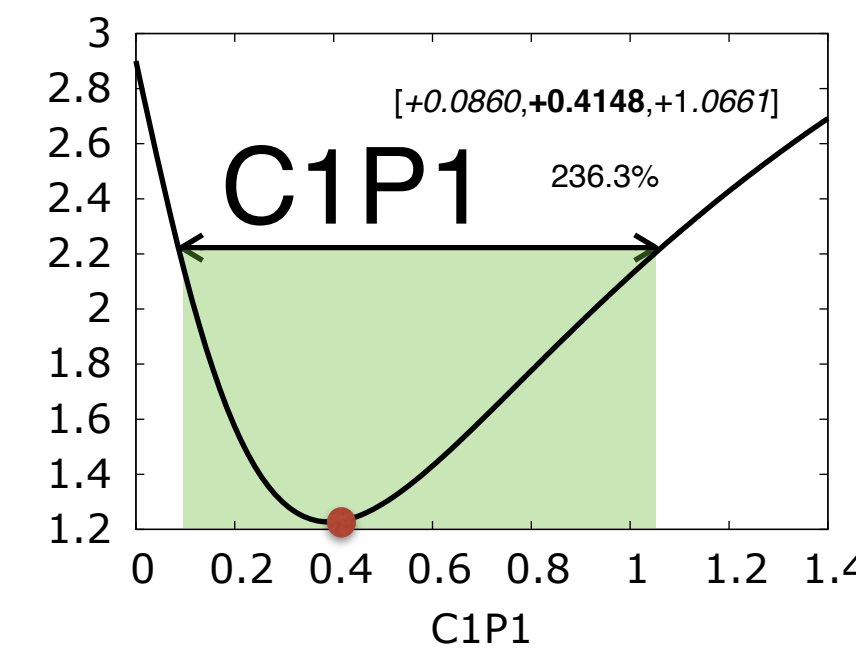
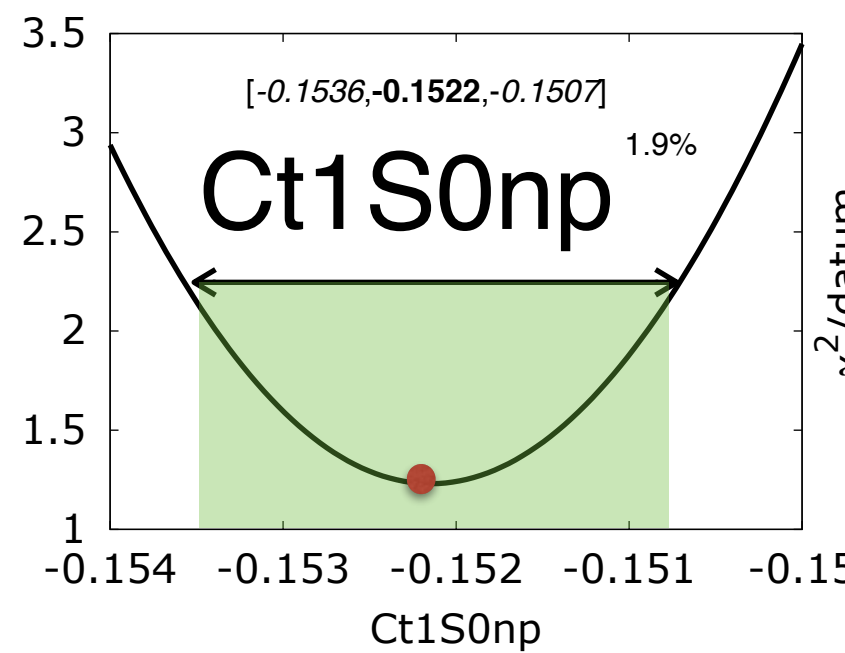
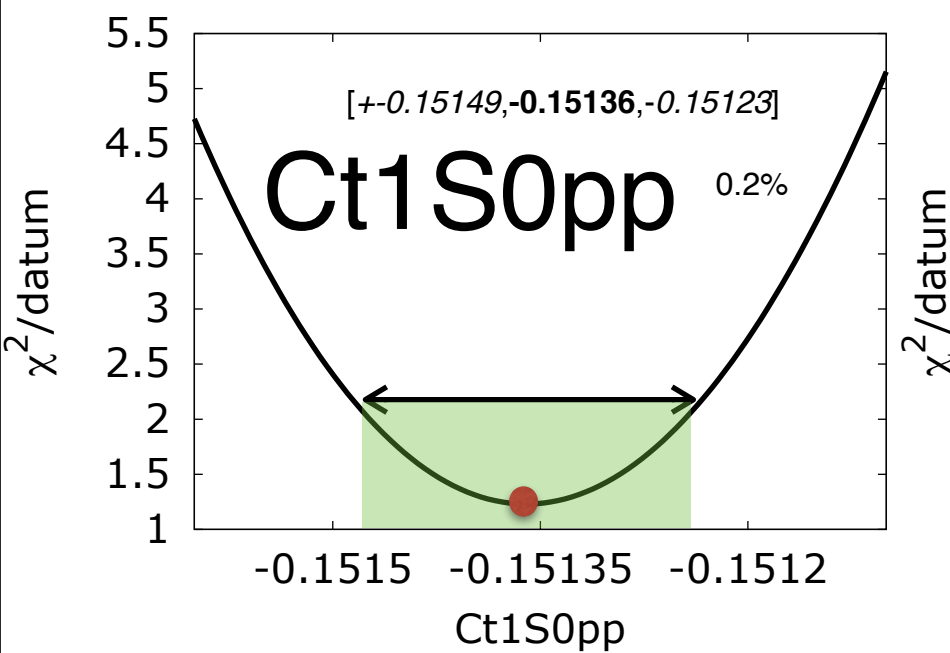
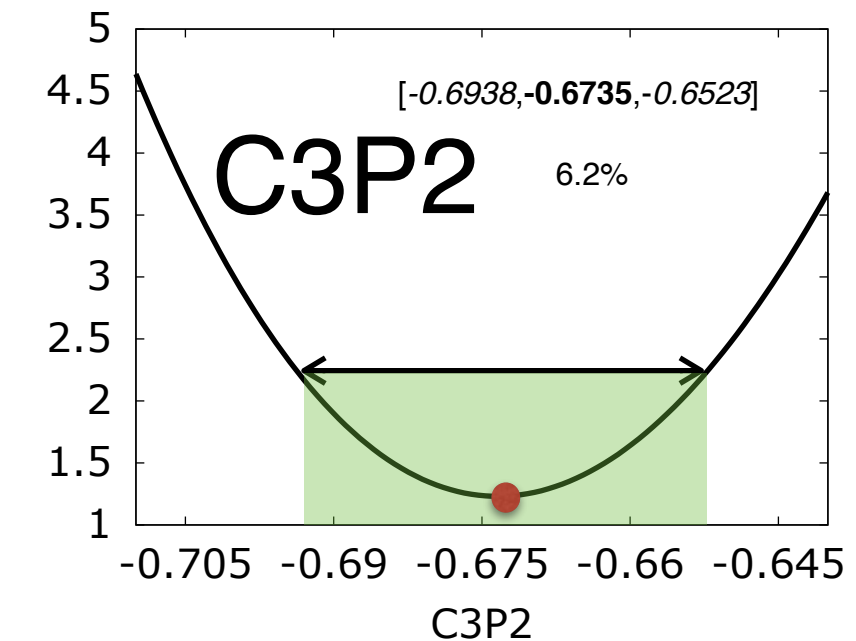
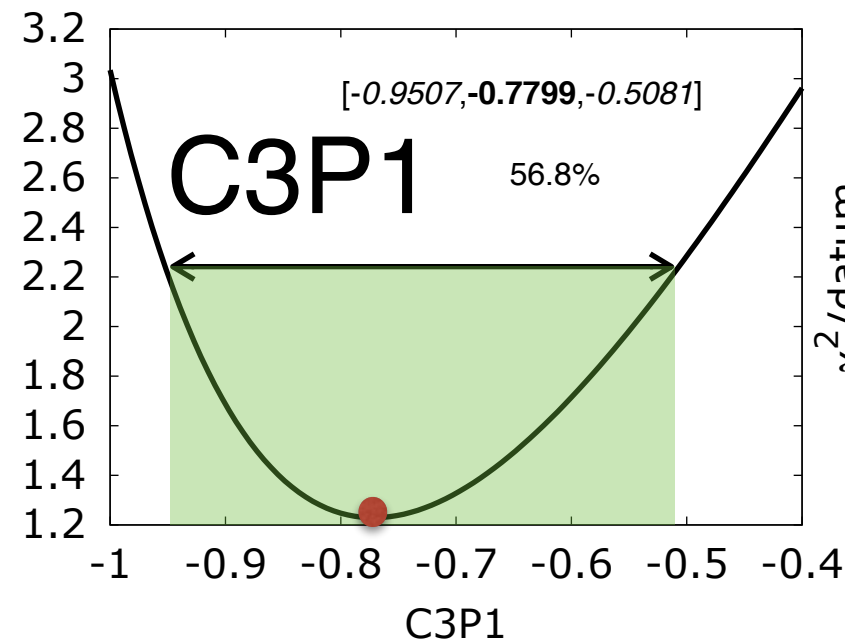
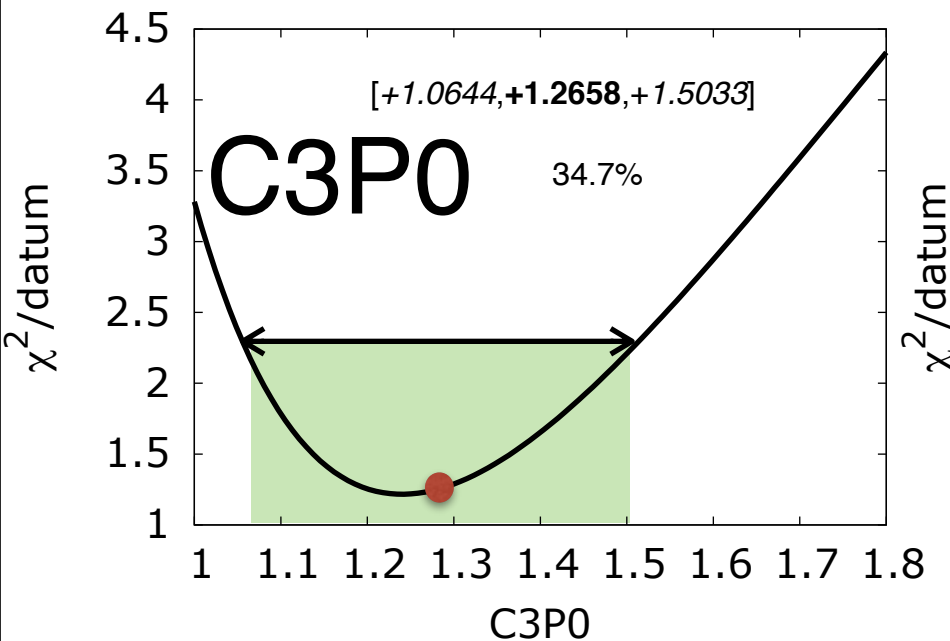
NNLOopt ($T_{\text{lab}} < 125$) uncertainty estimates



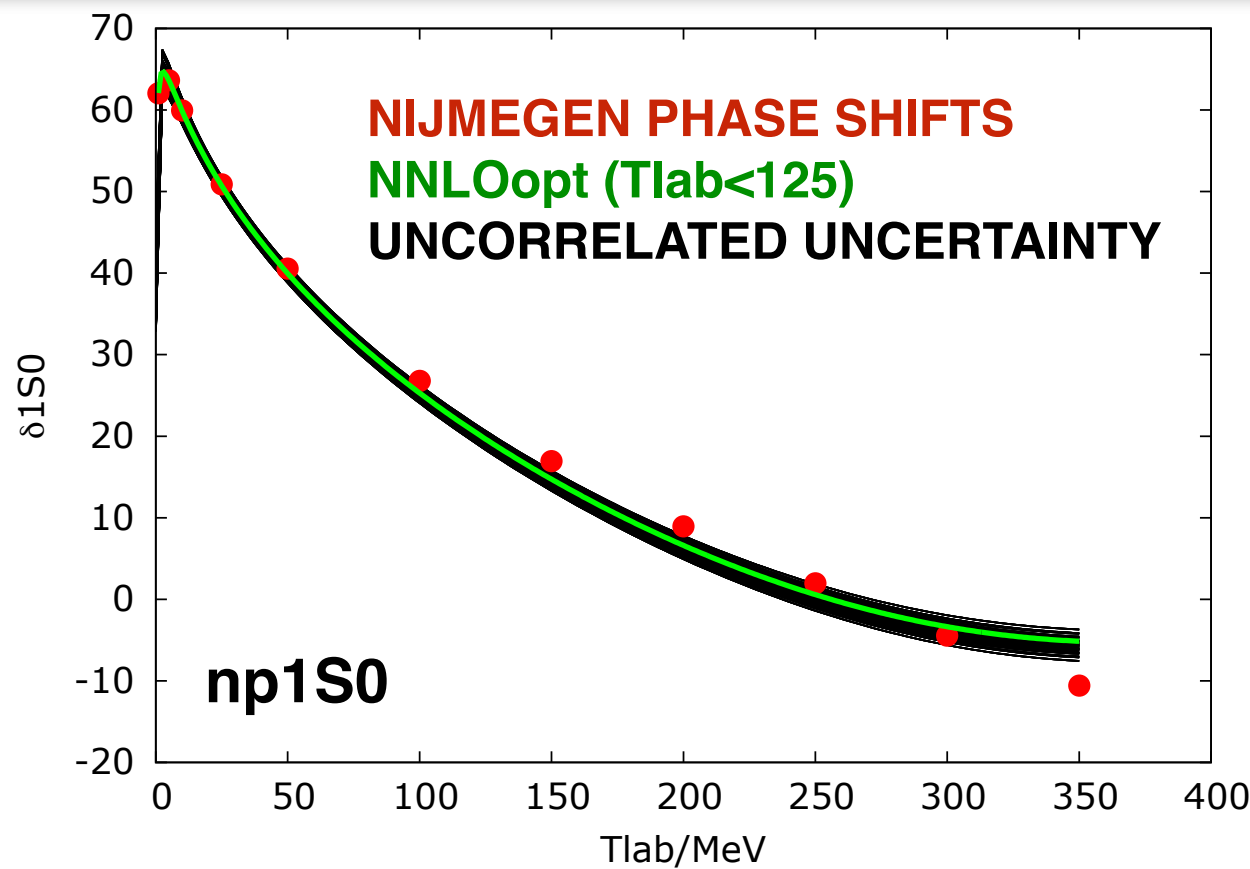
```
+++++
DEUTERON PROPERTIES
+++++
BINDING ENERGY      =      -2.224574962 MeV
RADIUS              =      1.967946562 fm
QUADRUPOLE MOMENT   =      0.271759995 fm2
D-STATE PROBABILITY =      4.039839760 %
```

At NNLO(500): The point in parameter space that reproduces the deuteron properties is within the uncertainty estimate. The optimum is slightly less bound.

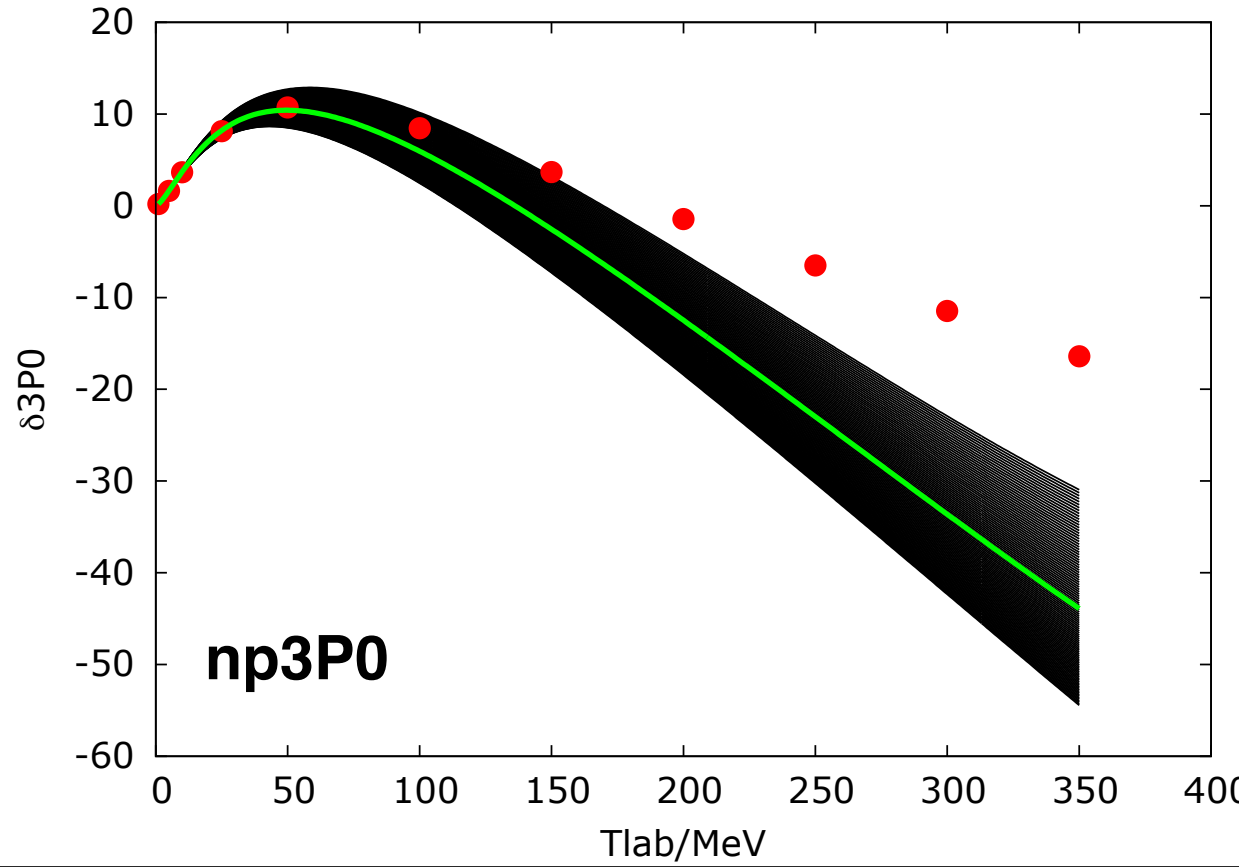
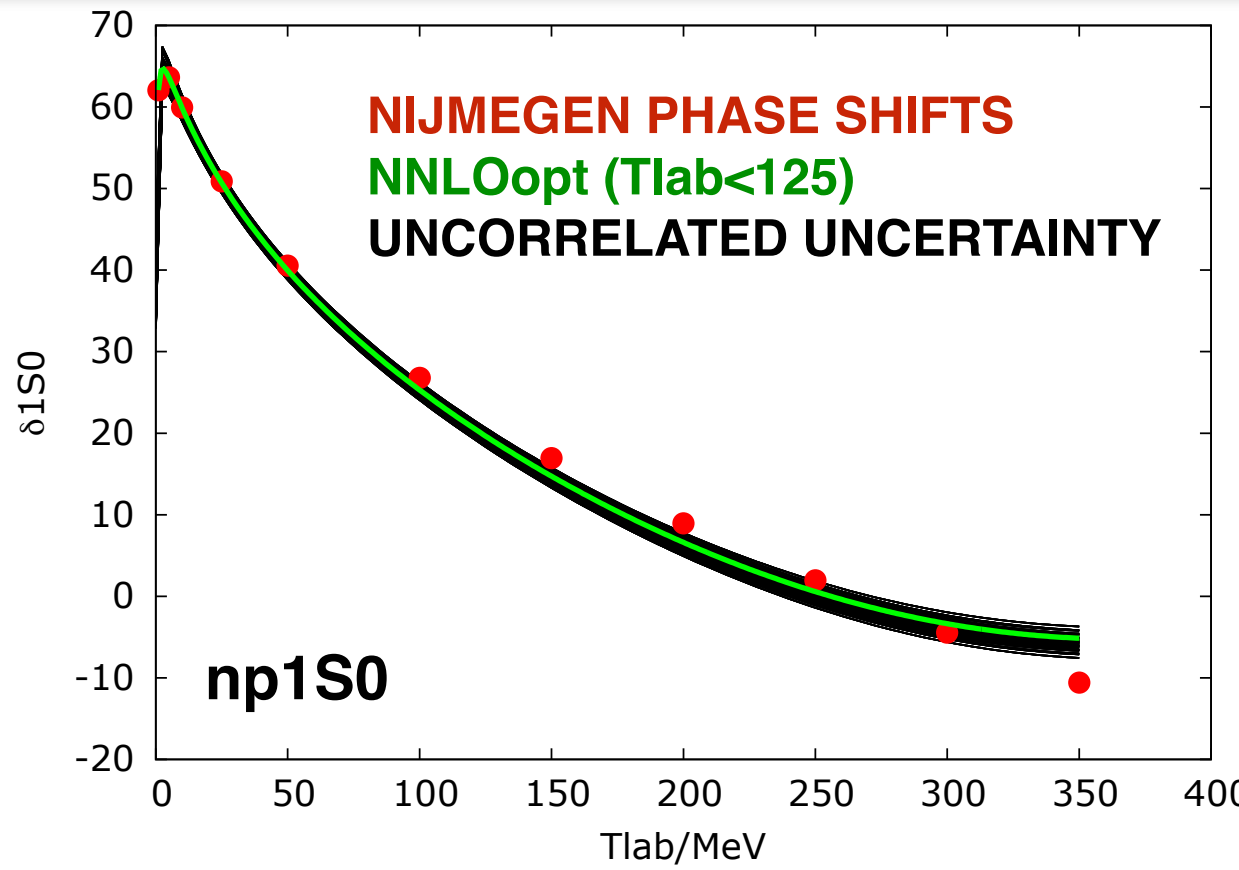
NNLOopt ($T_{\text{lab}} < 125$) uncertainty estimates



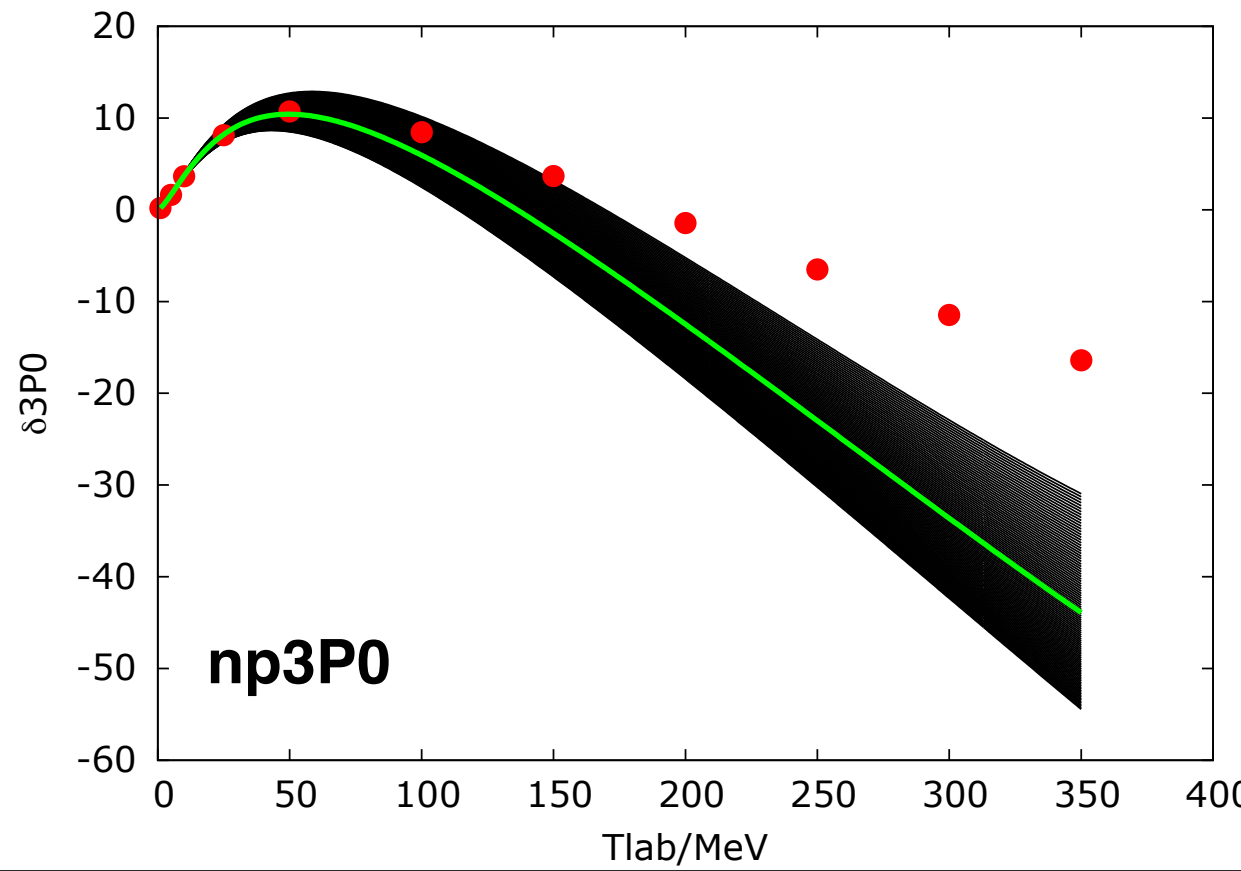
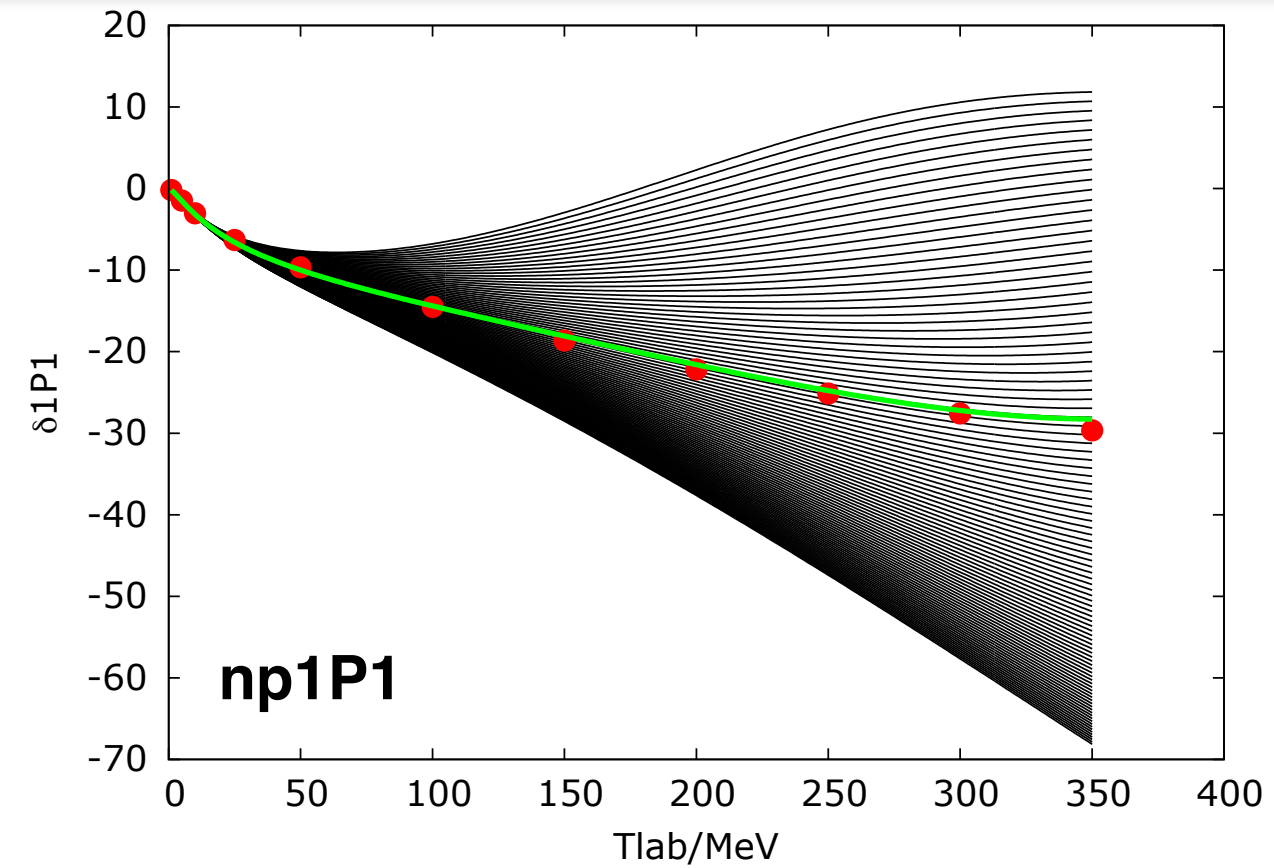
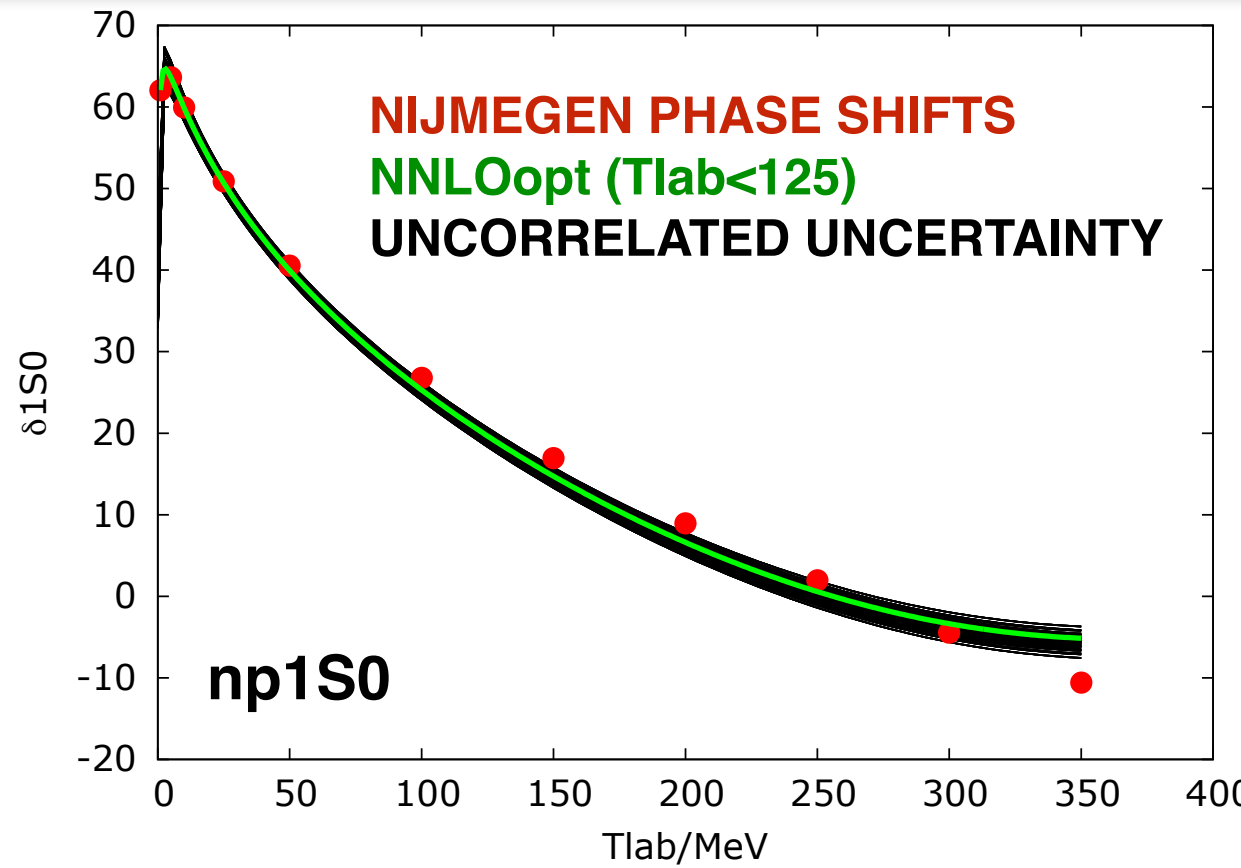
Phase shift sensitivity



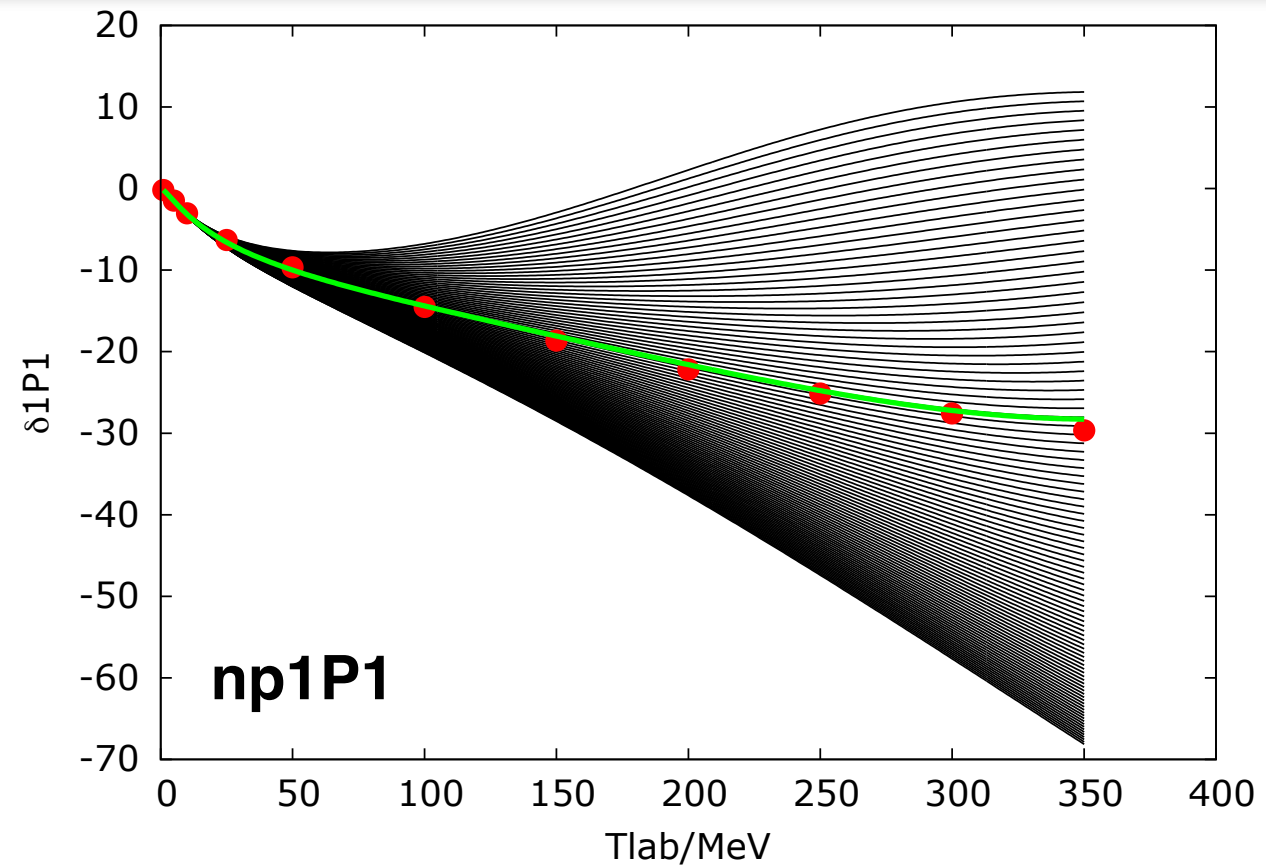
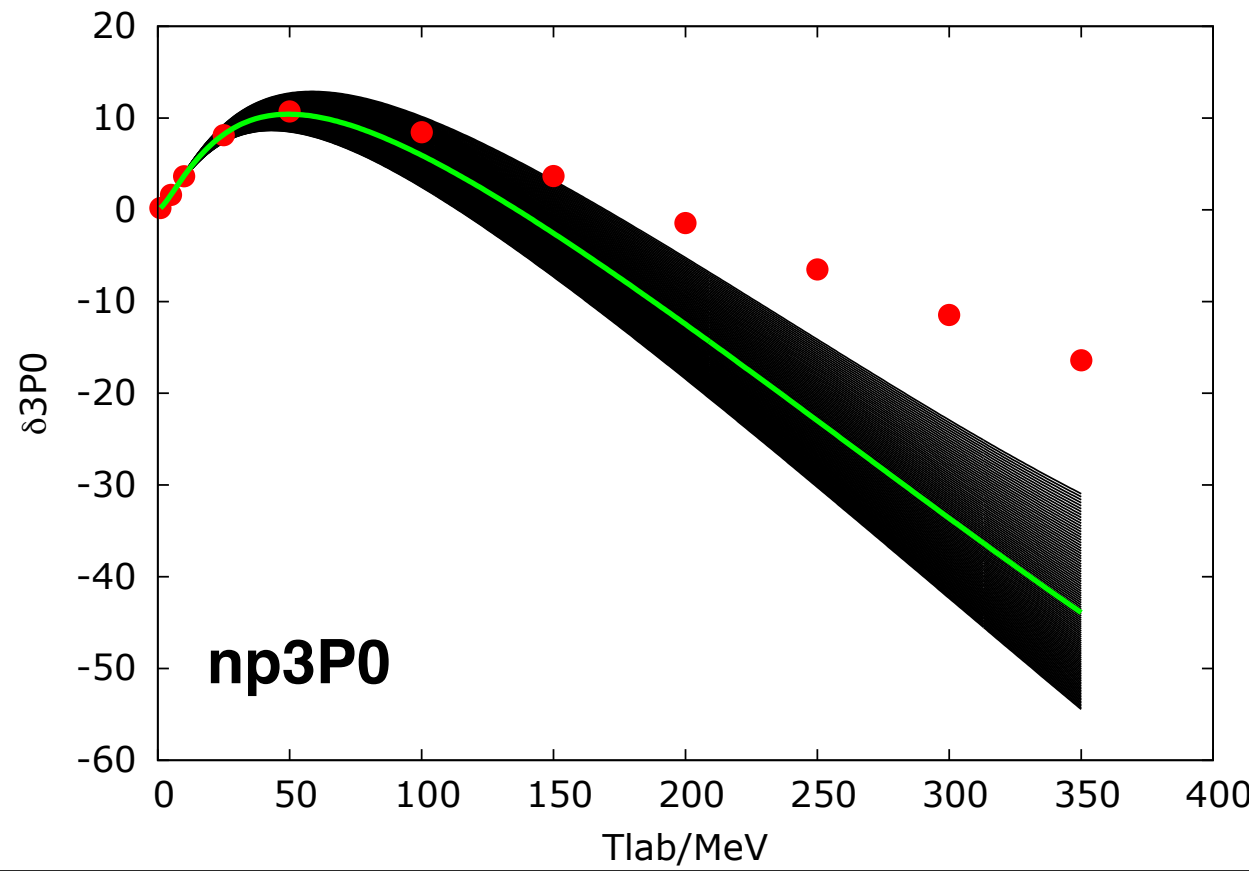
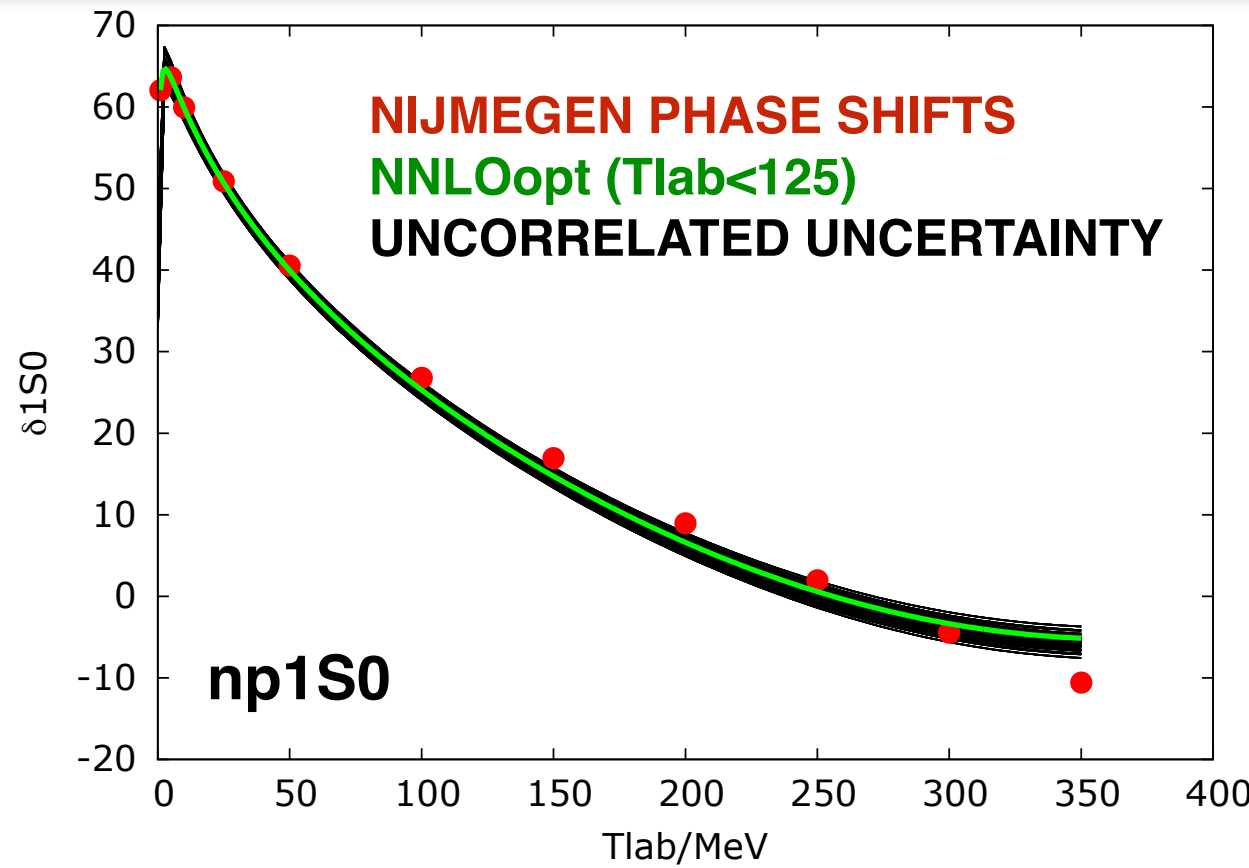
Phase shift sensitivity



Phase shift sensitivity

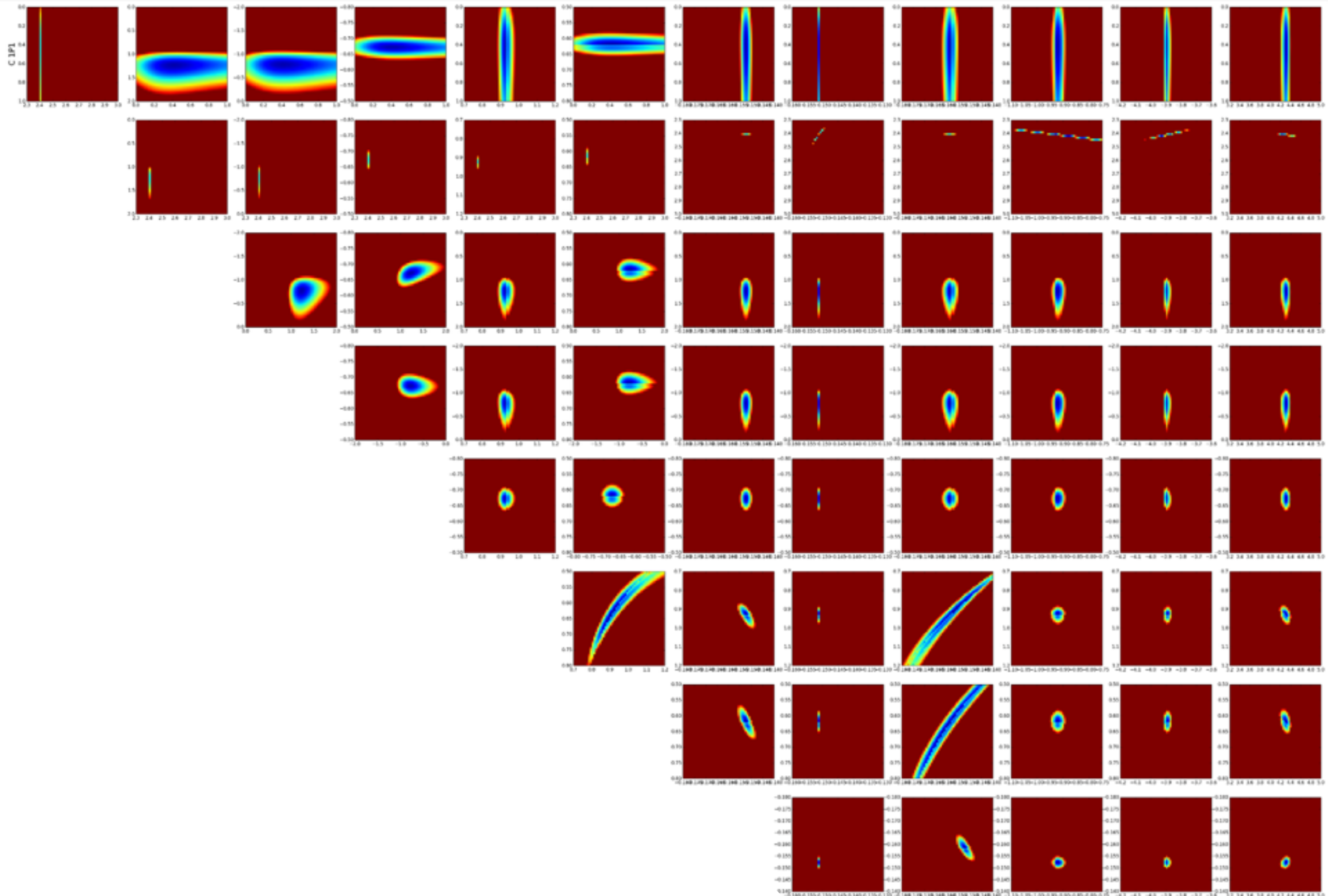


Phase shift sensitivity



IS0: well reproduced.
3P0: sensitive to data and impossible to reproduce above 125 MeV at NNLO
1P1: data beyond 125 MeV very important for constraining the uncertainty.

Correlations will be important



Summary

The expanded objective function can generate N2LO interactions that simultaneously describe the ground state energy and radii in the oxygen isotopic chain.

POUNDerS shows great promise to deliver state-of-the-art optimized nuclear forces for practical calculations.

The piN LECs require a careful analysis, and might be attributed with large uncertainties.

Outlook: Correlated uncertainty estimates.

Collaboration



UNIVERSITY
OF OSLO

University
of Idaho

Argonne
NATIONAL LABORATORY

THE UNIVERSITY OF
TENNESSEE 

OAK
RIDGE
National Laboratory

MICHIGAN STATE
UNIVERSITY



CHALMERS



NSCL

Collaboration

Gustav Baardsen

Boris Carlsson

Christian Forssen

Gaute Hagen

Morten Hjorth-Jensen

Gustav Jansen

Ruprecht Machleidt

Witold Nazarewicz

Thomas Papenbrock

Jason Sarich

Kyle Wendt

Stefan Wild



UNIVERSITY
OF OSLO

University
of Idaho

Argonne
NATIONAL LABORATORY

THE UNIVERSITY OF
TENNESSEE

OAK
RIDGE
National Laboratory

MICHIGAN STATE
UNIVERSITY



CHALMERS



NSCL

thank you for your attention!

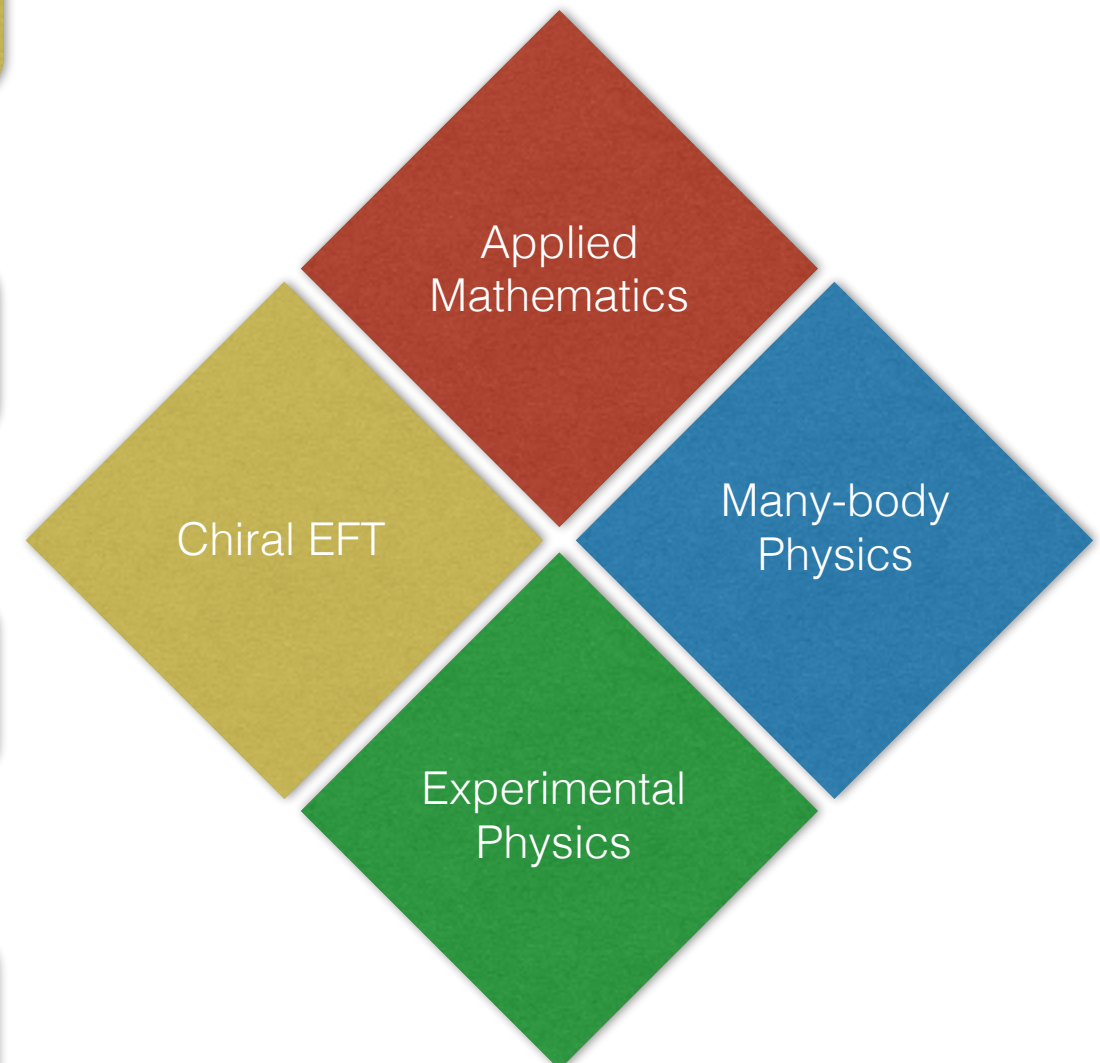
Optimization strategy

Set the parameters \mathbf{x} of the NN interaction

Compute phase shifts or observable
(currently: also $A=3,4$ ground state + radius)

Evaluate the objective function $f(\mathbf{x})$

Take new step in parameter space



Optimization strategy

Set the parameters \mathbf{x} of the NN interaction

LO,..,N3LO
NNN & piN
available

Compute phase shifts or observable
(currently: also A=3,4 ground state + radius)

Evaluate the objective function $f(\mathbf{x})$

Take new step in parameter space

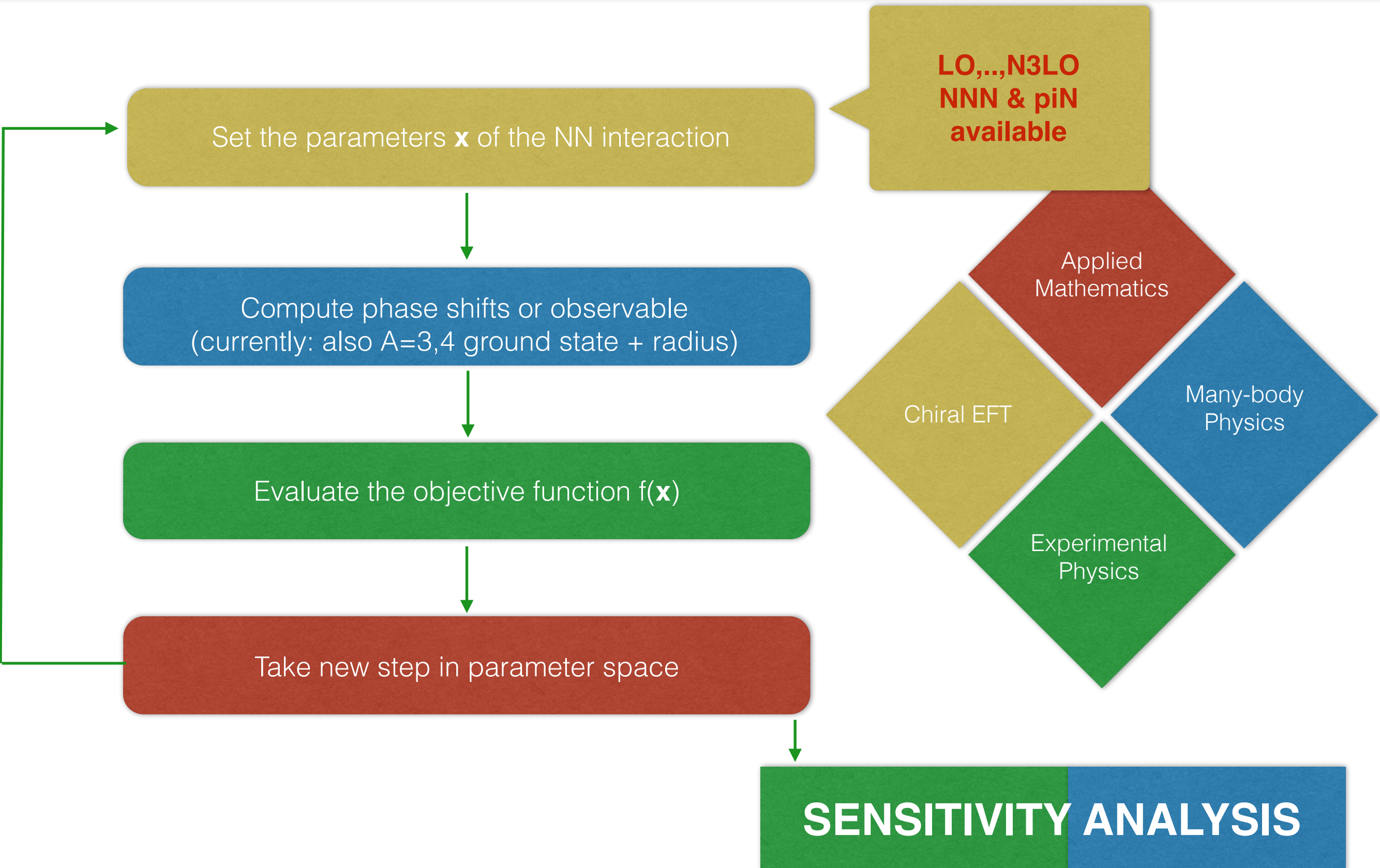
Applied
Mathematics

Chiral EFT

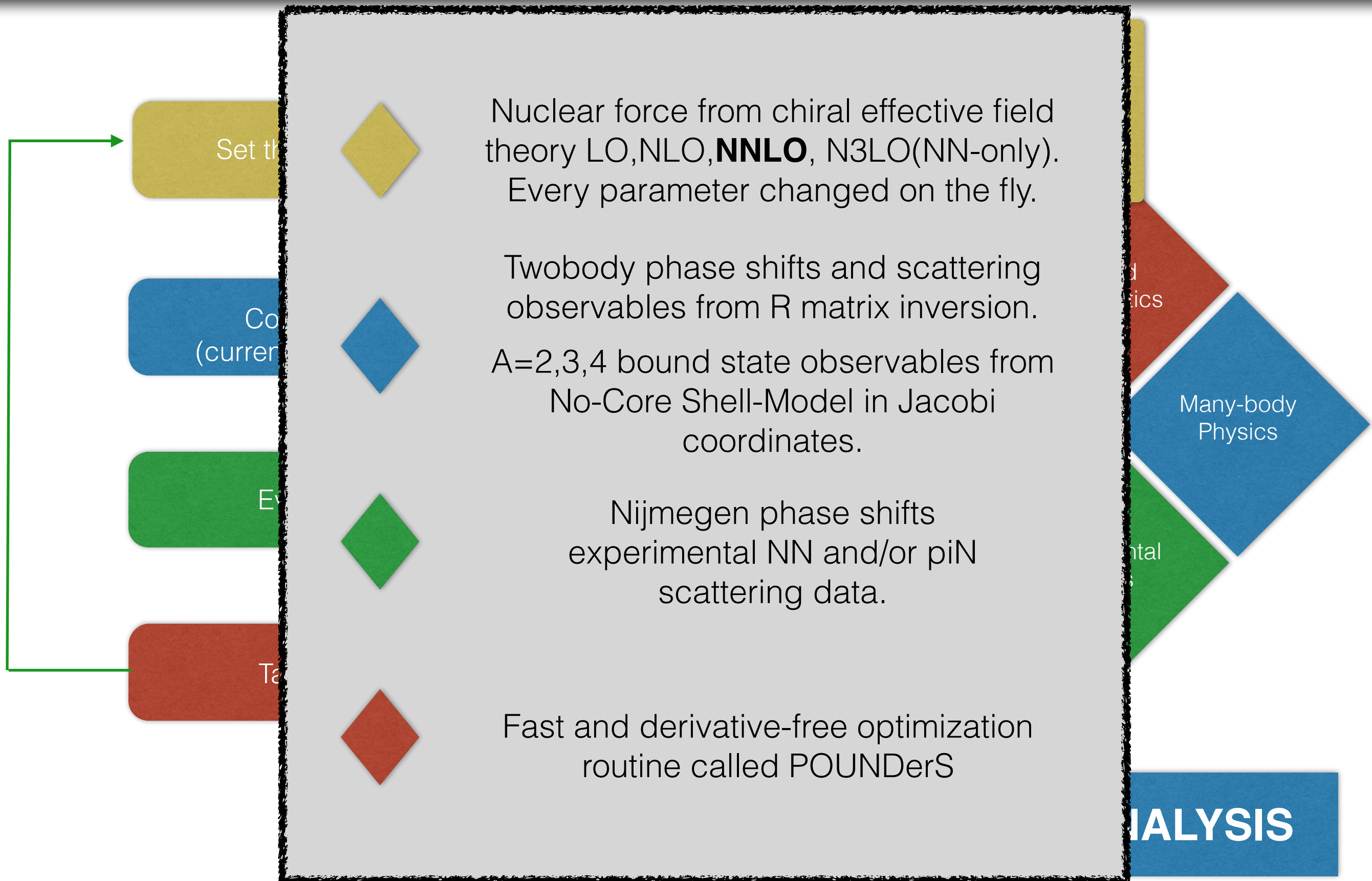
Many-body
Physics

Experimental
Physics

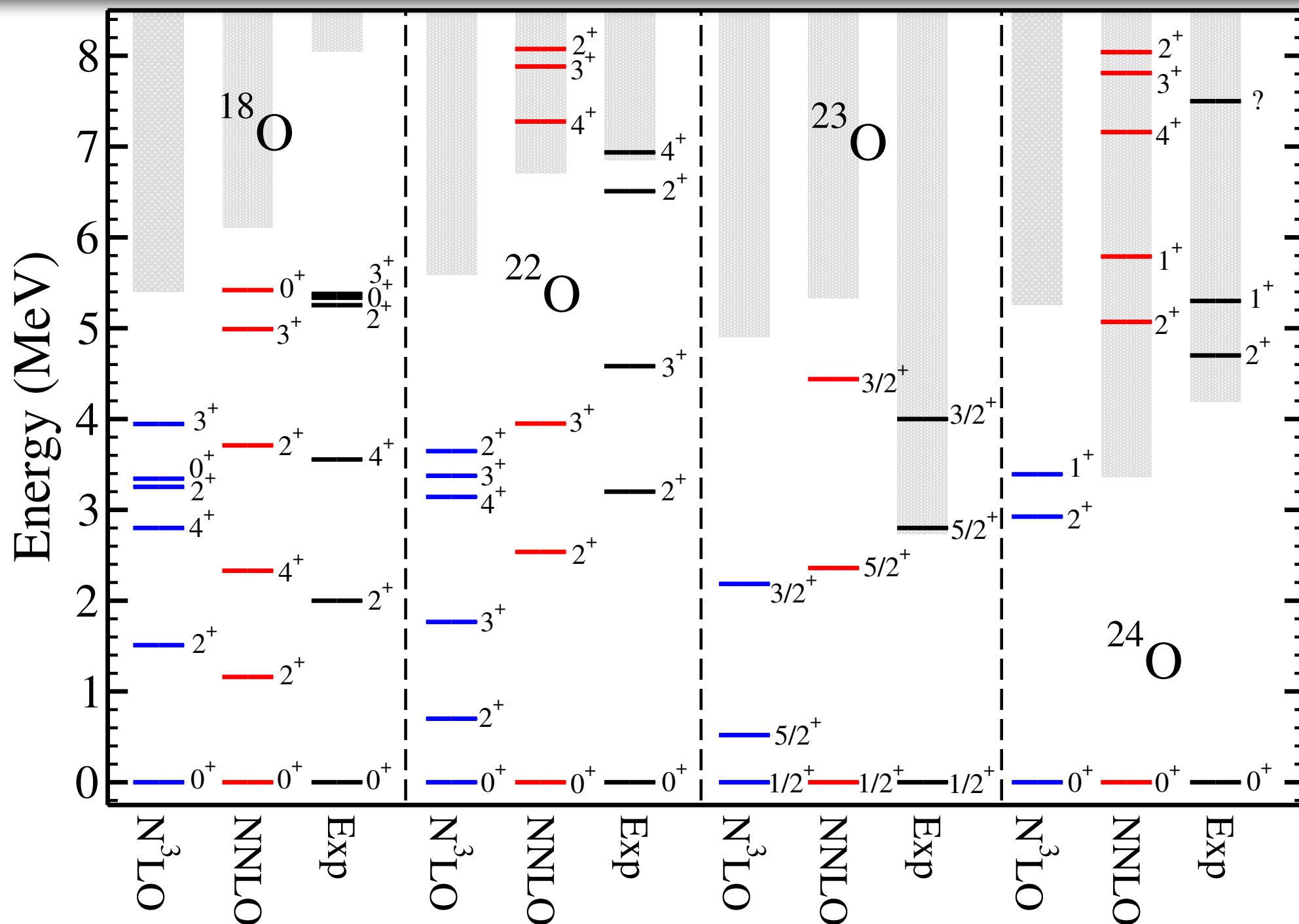
Optimization strategy



Optimization strategy



Oxygen excitation energies from NNLOopt



Oxygen24	2+	1+	4+	3+
NNLOopt	5.06	5.79	7.17	7.82
NNLO(EGM 450/500)	9.62	10.54	12.78	13.35
Experiment	4.7	5.3	?	?